

285
10/25/78

Sl. 720

DOE/JPL/954334-6

LOW COST SILICON SOLAR ARRAY PROJECT

Feasibility of Low-Cost, High-Volume Production of Silane and Pyrolysis
of Silane to Semiconductor-Grade Silicon

Quarterly Progress Report, January—March 1978

By

W. C. Breneman

E. G. Farrier

H. Morihara

Work Performed Under Contract No. NAS-7-100-954334

Union Carbide Corporation
Tarrytown, New York



U. S. Department of Energy

MASTER



Solar Energy

DISTRIBUTION OF THIS DOCUMENT IS UNLIMITED.

DISCLAIMER

This report was prepared as an account of work sponsored by an agency of the United States Government. Neither the United States Government nor any agency Thereof, nor any of their employees, makes any warranty, express or implied, or assumes any legal liability or responsibility for the accuracy, completeness, or usefulness of any information, apparatus, product, or process disclosed, or represents that its use would not infringe privately owned rights. Reference herein to any specific commercial product, process, or service by trade name, trademark, manufacturer, or otherwise does not necessarily constitute or imply its endorsement, recommendation, or favoring by the United States Government or any agency thereof. The views and opinions of authors expressed herein do not necessarily state or reflect those of the United States Government or any agency thereof.

DISCLAIMER

Portions of this document may be illegible in electronic image products. Images are produced from the best available original document.

NOTICE

This report was prepared as an account of work sponsored by the United States Government. Neither the United States nor the United States Department of Energy, nor any of their employees, nor any of their contractors, subcontractors, or their employees, makes any warranty, express or implied, or assumes any legal liability or responsibility for the accuracy, completeness or usefulness of any information, apparatus, product or process disclosed, or represents that its use would not infringe privately owned rights.

This report has been reproduced directly from the best available copy.

Available from the National Technical Information Service, U. S. Department of Commerce, Springfield, Virginia 22161.

Price: Paper Copy \$6.00
Microfiche \$3.00

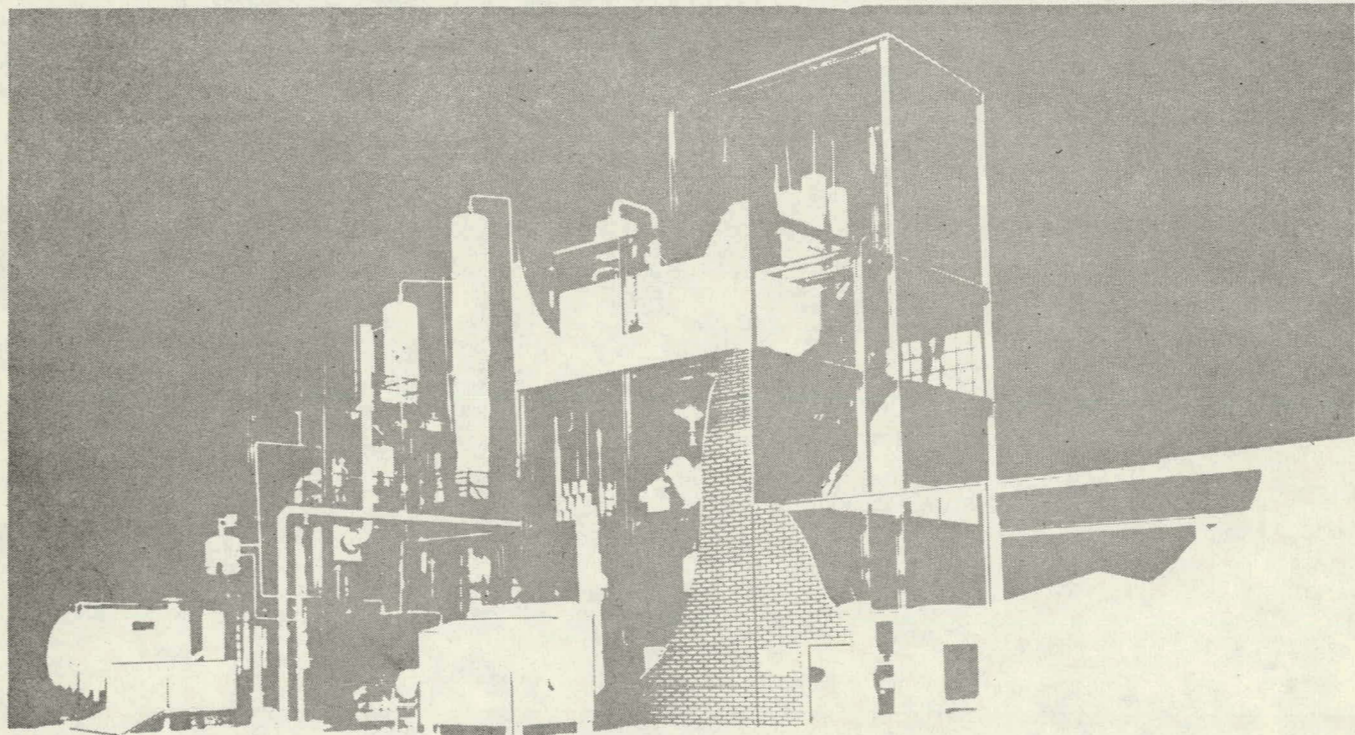
NOTICE
This report was prepared as an account of work sponsored by the United States Government. Neither the United States nor the United States Department of Energy, nor any of their employees, nor any of their contractors, subcontractors, or their employees, makes any warranty, express or implied, or assumes any legal liability or responsibility for the accuracy, completeness or usefulness of any information, apparatus, product or process disclosed, or represents that its use would not infringe privately owned rights.

QUARTERLY PROGRESS REPORT

January-March, 1978

low cost silicon solar array project

FEASIBILITY OF LOW-COST, HIGH-VOLUME PRODUCTION OF SILANE
AND PYROLYSIS OF SILANE TO SEMICONDUCTOR-GRADE SILICON



W.C. Breneman E.G. Farrier H. Morihara

**UNION CARBIDE
CORPORATION**

DISTRIBUTION OF THIS DOCUMENT IS UNLIMITED

88

ACKNOWLEDGEMENT

THE CONTRIBUTIONS OF THE FOLLOWING INDIVIDUALS
ARE GRATEFULLY RECOGNIZED:

R. K. BANSAL	F. S. DiPAOLO	E. J. McHALE
R. A. BEDDOME	G. L. DOYLE	I. NEMET
W. E. BeVIER	W. A. DRAPER, Jr.	R. L. OCHELTREE
H. CHEUNG	R. J. DUFALA	J. OROURKE
T. E. CHILDRESS	R. N. FLAGELLA	J. REXER
L. M. COLEMAN	S. K. IYA	L. J. SZELIGA
T. E. DIEGELMAN	K. C. KATHER	P. J. TIMMEL, Jr.

TABLE OF CONTENTS

	PAGE
ABSTRACT	1
1.0 SILANE PRODUCTION	4
1.1 INTRODUCTION	4
1.2 DISCUSSION	6
1.2.1 HYDROGEN STUDIES	6
1.2.2 THERMODYNAMIC ANALYSIS of the H-Si-Cl SYSTEM	15
1.2.3 INTEGRATED PROCESS OPERATION	18
1.3 CONCLUSIONS	20
1.4 PROJECTED QUARTERLY ACTIVITIES	21
1.5 REFERENCES	23
2.0 SILICON PRODUCTION	24
2.1 INTRODUCTION	24
2.2 DISCUSSION	25
2.2.1 SILANE PYROLYSIS	25
2.2.1a FLUID BED REACTOR	25
2.2.1b FREE SPACE REACTOR	28
2.2.2 SILICON CONSOLIDATION	31
2.3 CONCLUSIONS	32
2.4 PROJECTED QUARTERLY ACTIVITIES	33
2.4.1 FLUID BED REACTOR	33
2.4.2 FREE SPACE REACTOR	34
2.4.3 SILICON CONSOLIDATION	34
2.5 REFERENCES	35
3.0 PROCESS DESIGN	36
3.1 INTRODUCTION	36
3.2 DISCUSSION	37
3.2.1 PROCESS SPECIFICATIONS UPDATE	37
3.2.2 KEY EQUIPMENT DESIGN for the 25 MT/YR FACILITY	40
3.2.2a HYDROGENATION	40
3.2.2b REDISTRIBUTION	40
3.2.2c DISTILLATION	41
3.2.2d ADSORPTION	43
3.2.2e PYROLYSIS/MELTING	44

TABLE OF CONTENTS (Cont'd)

	PAGE
3.2.3 SGS PROCESS DESIGN PACKAGE for the 25 MT/YR FACILITY	47
3.2.4 SGS PROCESS DESIGN for a 1000 MT/YR COMMERCIAL PLANT	48
3.2.4a PROCESS FLOW DIAGRAM	48
3.2.4b SCALE MODEL	54
3.2.5 PRELIMINARY COSTS of 25, 50, 100 and 1000 MT/YR PLANTS	54
3.2.6 PROCESS DESIGN DATA	58
3.2.6a PHYSICAL and CRITICAL PROPERTIES of SILANE and CHLOROSILANES	58
3.2.6b PROCESS DESIGN DATA ACQUISITION	60
3.3 CONCLUSIONS	61
3.4 PROJECTED QUARTERLY ACTIVITIES	62
3.4.1 PRELIMINARY PROCESS DESIGN of 25 MT/YR EXPERIMENTAL FACILITY	62
3.4.2 FINAL PROCESS DESIGN of EXPERIMENTAL FACILITY	62
3.4.3 RESEARCH and DEVELOPMENT PROGRAM PLAN	62
3.5 REFERENCES	63
4.0 CAPACITIVE FLUID-BED HEATING	64
4.1 INTRODUCTION	64
4.2 DISCUSSION	65
4.2.1 ANALYTICAL MODEL	65
4.2.2 EXPERIMENTAL STUDY	69
4.2.2a FLUIDIZATION CHARACTERISTICS	69
4.2.2b ELECTRICAL PHENOMENA	69
4.2.2c TEMPERATURE MEASUREMENT	73
4.3 CONCLUSIONS	76
4.4 PROJECTED QUARTERLY ACTIVITIES	77
4.4.1 EXPERIMENTAL INVESTIGATION	77
4.4.2 ANALYTICAL WORK	77

ILLUSTRATIONS

FIGURE NO.	TITLE	PAGE
1.1	SCANNING ELECTRON MICROGRAPH of REACTED COPPER TURNINGS	9
1.2	HYDROGENATION of SiCl_4 to HSiCl_3 at 500°C	10
1.3	HYDROGENATION of SiCl_4 to HSiCl_3 at 450°C	12
1.4	HYDROGENATION of SiCl_4 to HSiCl_3 at 500°C with and without COPPER CATALYST	13
1.5	SCANNING ELECTRON MICROGRAPH of REACTED Cu/Si CONTACT MASS	14
1.6	HEATS of FORMATION of HYDROCHLOROSILANES	17
1.7	HSiCl_3 DISPROPORTIONATION UNIT	19
2.1	PHOTOMICROGRAPH of CROSS-SECTIONED PARTICLES COATED in the FLUID BED REACTOR	26
2.2	SILICON GROWTH of FLUID BED REACTOR GAS-INJECTION SYSTEM	26
3.1	DISTILLATION COLUMN DESIGN for the 25 MT/YR EXPERIMENTAL FACILITY	42
3.2	25 MT/YR EXPERIMENTAL FACILITY SILANE PYROLYSIS and POWDER MELTING APPARATUS	45
3.3	PRELIMINARY SGS PROCESS FLOW DIAGRAM for 1000 MT/YR PLANT, SHEET 1	49
3.3	SHEET 2	50
3.3	SHEET 3	51
3.4	PLOT PLAN for the 1000 MT/YR SGS PLANT	55
3.5	SCALE MODEL of the 1000 MT/YR SGS PLANT	56
4.1	CRITICAL SILANE CONCENTRATION vs. TEMPERATURE	67
4.2	POWER REQUIREMENT per KILOGRAM PRODUCT vs. TEMPERATURE of PARTICLE	67
4.3	BED DEPTH vs. TEMPERATURE for 99% CONVERSION of SILANE to SILICON	68
4.4	REACTOR DIAMETER vs. BED TEMPERATURE	68
4.5	MINIMUM FLUIDIZATION VELOCITY vs. EFFECTIVE PARTICLE DIAMETER for SILICON PARTICLES	72
4.6	CURRENT vs. FREQUENCY of BED in STATE H	72

ILLUSTRATIONS (Cont'd)

FIGURE NO.	TITLE	PAGE
4.7	CURRENT vs. FREQUENCY of BED in STATE L	74
4.8	SKETCH of COATED ELECTRODE	74
4.9	THERMAL vs. ELECTRICAL POWER	75
4.10	MAXIMUM TEMPERATURE DIFFERENCE in BED NORMALIZED to INPUT POWER vs. FLOW VELOCITY NORMALIZED to MINIMUM FLUIDIZATION VELOCITY	75

TABLES

TABLE NO.	TITLE	PAGE
1.1	ACTIVATION ENERGIES in HYDROGENATION of SiCl_4	7
1.2	BORON ANALYSIS around HSiCl_3 UNIT	20
2.1	PROPERTIES of VACUUM MELTED and CAST PELLETS	32
3.1	PYROLYSIS/MELTING PARTS LIST for 25 MT/YR PLANT	46
3.2	PRODUCT COST from a 1000 MT/YR SGS COMMERCIAL PLANT	57
3.3	PRODUCT COSTS for VARIOUS PLANT SIZES, FINANCES	59
4.1	OBSERVED FLUIDIZATION CHARACTERISTICS of a BED	70
4.2	OBSERVED and PREDICTED MINIMUM FLUIDIZATION VELOCITIES	71

ABSTRACT

SILANE PRODUCTION

Studies on the hydrogenation of silicon tetrachloride have shown this reaction to be mildly endothermic (8-9 kcal/mole) with a modest activation energy of about 10 kcal/mole. Bulk copper catalyst concentration does not strongly affect reaction kinetics, and indications are that diffusion is an important kinetic resistance. The apparent equilibrium shift of H-Si-Cl system in the presence or absence of silicon and/or copper catalyst and the effect of reaction on the Cu/Si surface, suggest that hydrogenation is probably a complicated reaction sequence. Copper chloride is a likely transient intermediate and hydrogen chloride may be an active intermediate.

Thermodynamic analysis of the H-Si-Cl system has been performed to serve as a basis for scale up of the various reactions. While the heats of formation of most of the H_xSiCl_{4-x} compounds agree reasonably well with published values, a significant discrepancy was noted for H_3SiCl . The analysis indicates thermal effects in the disproportionation reactions are minor.

The silane process development unit (PDU) was operated in order to demonstrate the closed cycle production of silane via hydrogenation and disproportionation. Integration of the $HSiCl_3$ disproportionation reactor and fractionating column with the hydrogenation reactor and silane units was accomplished. The trichlorosilanes-to-dichlorosilane unit met the design standards of 20 mole percent equilibrium conversion of $HSiCl_3$, and a material balance around the hydrogenation unit showed a silicon utilization efficiency of 84%. Results of analysis of the $HSiCl_3$ reactor inlet and outlet, and of the $HSiCl_3$ still distillate indicate boron levels well below the acceptable range for this part of the system. Start-up of the silane unit revealed several minor piping changes that were needed to assure reliable operation. Data obtained to date indicate a close agreement between the design and operation of the PDU.

SILICON PRODUCTION

Silane, diluted with helium, was injected into a quartz fluid-bed reactor in a series of preliminary equipment evaluation experiments. Experiments were conducted for up to two hours with no observable silicon or silane reaction occurring with the reactor walls and without locking up the bed. The range of gas velocities that sustained a stable fluidized bed was studied at various temperatures and bed depths for -35/+60 mesh particles. Stable fluidized beds were obtained at room temperature over a wide range of gas velocities. The gas velocity range capable of maintaining a stable fluidized bed at 950°C was reduced to one-fourth that obtained at room temperature. The elevated temperature data were in good

agreement with calculated values for onset of fluidization and for the behavior predictable from the thermal expansion of the fluidizing gas.

Silane was converted into silicon powder at a rate of 0.45 kg/hr for eight continuous hours as a partial demonstration of the capability of the free space reactor. The powder was subsequently pneumatically transferred from the free space reactor to a melt consolidation apparatus and melted in a commercial grade quartz crucible at an average rate of 1.14 kg/hr. A dross-free casting was obtained.

Semi-conductor grade silicon and free space reactor powder were vacuum-melted and cast into pellets in standard grade quartz. The electrical resistivities were 30 ohm-cm and 20 ohm-cm, respectively. A pellet cast from melted free space reactor powder, into a high purity quartz crucible, had an electrical resistivity of 120 ohm-cm. The pellet samples were forwarded to JPL for purity analysis. A free space reactor powder sample was also sent with the cast pellets.

Thermodynamic calculations indicated that an adiabatic conversion of silane-to-silicon may occur at 400°C. Kinetic data indicated that the reaction rate at that temperature was too slow to support an efficient decomposition reaction in the current free space reactor. Efficient silane pyrolyses were not obtained with the current reactor configuration at reactor wall temperatures below 800°C.

PROCESS DESIGN

The major goal for this quarter was to assemble an SGS (semiconductor-grade silane/silicon) process design package for the 25 MT/Yr experimental facility. The package was generated and is undergoing final inspection. The process design effort began with the selection of the best process design scheme, which is a hybrid of the Adsorption Silane Process and the Distillation Silane Process.

In preparation for the process design package, a thorough examination of the design of key pieces of equipment was made. Detailed specifications for all major equipment were prepared and the equipment cost was acquired through vendor contacts and in-house manuals.

A preliminary process design and plant cost of a 1000 MT/Yr commercial facility were made a few months ahead of schedule at the request of JPL. The plant cost is estimated at \$6 million. The selling price of product from such a plant is expected to be well below the JPL/DOE 1986 cost goal of \$10/Kg. Plant costs for 25, 50, and 100 MT/Yr experimental facilities were also calculated by scaling from the 1000 MT/Yr plant estimate.

All necessary arrangements were completed for the in-house acquisition of key process design data. The experimental work will begin in April and all tests should be completed by September 1978. These data will be incorporated into the second iteration process design of the experimental facility.

CAPACITIVE FLUID-BED HEATING

Fluidization Regimes of various particle-size ranges were observed experimentally with nitrogen, argon, and helium. Experimental minimum fluidization velocities agree reasonably well with the predicted values. The bed was heated capacitively and the temperature variations within the bed were recorded. As predicted, the bed temperatures everywhere were essentially the same as long as the bed was fluidized.

A mathematical model for heterogeneous-decomposition of silane on the surface of silicon seed particles in a fluid-bed reactor was constructed. The model is based on epitaxial silicon deposition data (very dilute silane). It has been used to study various fluid-bed silane pyrolysis schemes from which a most promising one has been selected for a functional process design and cost estimate. The analysis indicates that if the bed temperature is low (say 950°K), the power input to the bed and the bed size are reasonable; however, the product may be porous and there is a possibility that the morphology may not be acceptable.

1.0 SILANE PRODUCTION

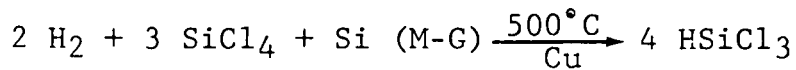
1.1 INTRODUCTION

The purpose of this program is to determine the feasibility and practicality of high-volume, low-cost production of silane (SiH_4) as an intermediate for obtaining solar-grade silicon metal. The process is based on the synthesis of SiH_4 by the catalytic disproportionation of chlorosilanes resulting from the reaction of hydrogen, metallurgical silicon, and silicon tetrachloride. The goal is to demonstrate the feasibility of a silane production cost of under \$4.00/kg at a production rate of 1000 MT/year.

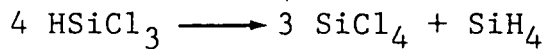
Prior to the inception of this program in October 1975, Union Carbide had shown that pure hydrochlorosilanes could be disproportionated to an equilibrium mixture of other hydrochlorosilanes by contact with a tertiary-amine, ion-exchange resin. In addition, Union Carbide had shown that silicon tetrachloride, a by-product of silane disproportionation, can be converted to trichlorosilane by reaction with metallurgical silicon metal and hydrogen.

Thus, a closed-cycle purification scheme was proposed to convert metallurgical-grade silicon into high-purity, solar-grade silicon using hydrochlorosilanes as intermediates. This process appears as:

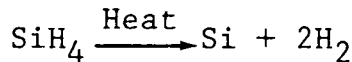
1. Hydrogenation of metallurgical silicon metal and of by-product silicon tetrachloride to form trichlorosilane.



2. Disproportionation of trichlorosilane to silane and silicon tetrachloride.



3. Pyrolysis of silane to high-purity silicon.



Until now, laboratory investigations have defined this rate, equilibrium conversion, and certain mechanistic aspects of the disproportionation and hydrogenation reactions at atmospheric pressure. A small process development unit, capable of operating under pressure, was constructed and operated to demonstrate the conversion of dichlorosilane to silane. The construction of a high-pressure hydrogenation unit and of an integrated silane unit was completed.

Last quarter, the kinetics of the hydrogenation reaction was studied at elevated pressures and a thermodynamic analysis of the H-Si-Cl system was performed. The integrated silane process development unit (PDU) was operated in order to demonstrate the closed cycle production of silane via hydrogenation and disproportionation.

1.2 DISCUSSION

1.2.1 HYDROGEN STUDIES

An estimate of the heat of reaction to form trichlorosilane and dichlorosilane by the reactions:



was made by plotting the variation of equilibrium constant with temperature. The heat of reaction was determined as the slope of the line, $\ln K_p$ versus $1/T$ using the least squares fit. The values of +8.3 and +9.1 kcal/mole Si are consistent with the observed increasing conversion at higher temperatures. These values do not agree with the JANAF tables^(2.0) but do agree with more recent data^(1.0) which give -116.9 kcal/g mole as the heat of formation of TCS compared to the JANAF value of -112 kcal/g mole.

Data obtained in the 3-inch diameter Process Development Unit (PDU) hydrogenation reactor were used to calculate the activation energy for reaction (1). In the fluidized bed reactor, for a given H_2/SiCl_4 ratio, pressure, % yield, and fluidization regime, it can be shown that:

$$[\text{Bed height}]_1 e^{-A/RT_1} = [\text{Bed height}]_2 e^{-A/RT_2} \quad (3)$$

Equation (3) was used to calculate activation energies for various conditions that were employed and the results are given

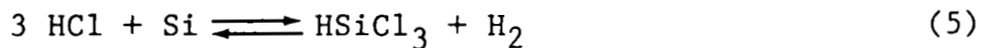
in Table 1.1. The low values for A indicate that diffusion may play a role in determining the rate of the hydrogenation reaction.

Table 1.1

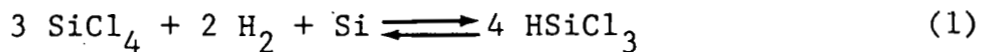
ACTIVATION ENERGIES IN HYDROGENATION OF SiCl_4

H_2/SiCl_4 Ratio	% Yield HSiCl_3	Bed Ht 1	Bed Ht 2	Activation Energy kcal/mole
2.0	15	17	27	21.3
2.0	15	27	36	8.6
5.0	20	27	36	6.4

Extensive studies of the reaction of SiCl_4 and HSiCl_3 with hydrogen at elevated temperatures have suggested a plausible overall mechanism for the hydrogenation reaction as



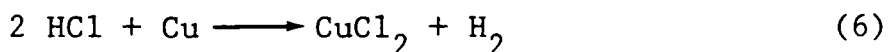
or an overall reaction of



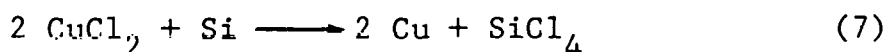
Reactions (4) and (5) are known to occur at some temperature. Whether reaction (4) is involved in the net reaction (1) at 500°C has not been established. The laboratory stainless steel reactor was thoroughly cleaned and the reaction of H_2 and SiCl_4 attempted in the empty tube at 500°C, 67 psia.

A small but significant amount of HSiCl_3 (about 2%) was formed at 58 seconds residence time and a H_2/SiCl_4 ratio of 1.3/1. The conversion to HSiCl_3 increased to 3% at a higher H_2/SiCl_4 ratio of 2.5/1.

The reaction above was repeated packing the tube with fine copper turnings. The results were essentially the same in that only about 1.7% HSiCl_3 was produced. Analysis of the vent gas indicated the presence of to 2% HCl which is the correct amount for the stoichiometry of reaction (4). Analysis of the copper metal by Scanning Electron Microscopy after reaction showed some etching of the copper metal surface, the presence of fine particles of copper chloride and a trace of silicon metal (Figure 1.1). The latter was present uniformly over the entire metal surface. However, there was no evidence of "polycrystalline silicon" growth on the copper metal surface. These findings show that in fact copper chloride could form in this environment according to the reaction:



Since it is known that copper chloride can also react with silicon metal in the presence of hydrogen at these temperatures:



a possible route for the formation of Si/Cu alloy can be explained.

According to thermodynamic considerations, the level of HSiCl_3 and HCl in the absence of silicon metal should be on the order of 5 mole % following the path of reaction (4). The found value of about 3% is close to that estimated value.

When reaction (4) is attempted in the presence of either silicon metal, or copper, HCl levels in the effluent would be reduced either through reaction (5) or (6). In the former case, a large increase in the HSiCl_3 level would also be expected.

Prior work^(3.0) in the 1" laboratory reactor utilized a 4% copper catalyst in the metallurgical silicon. To further explore the effect of copper, an evaluation was made using a 2% copper catalyst concentration. A plot of HSiCl_3 yield versus residence time (Figure 1.2) indicates the reaction path is nearly identical to that found in previous studies.

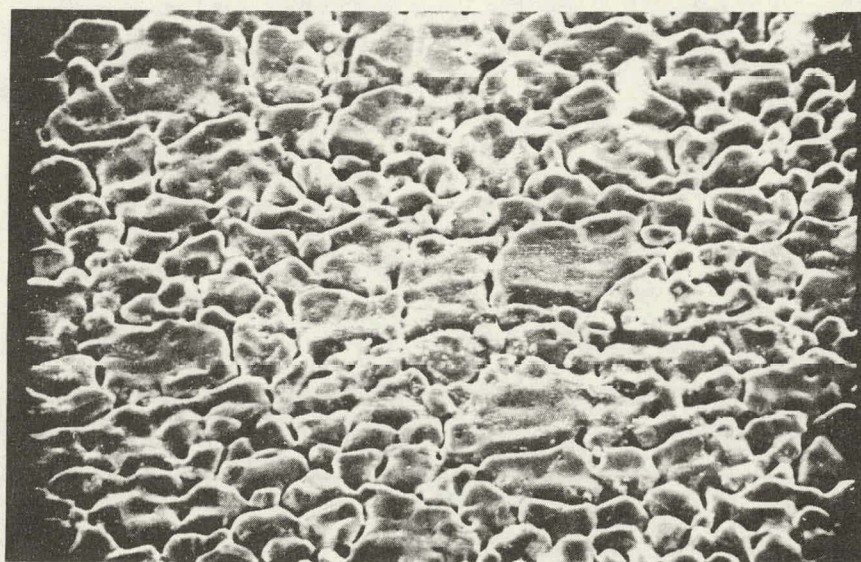


Figure 1.1

SCANNING ELECTRON MICROGRAPH
OF REACTED COPPER TURNINGS

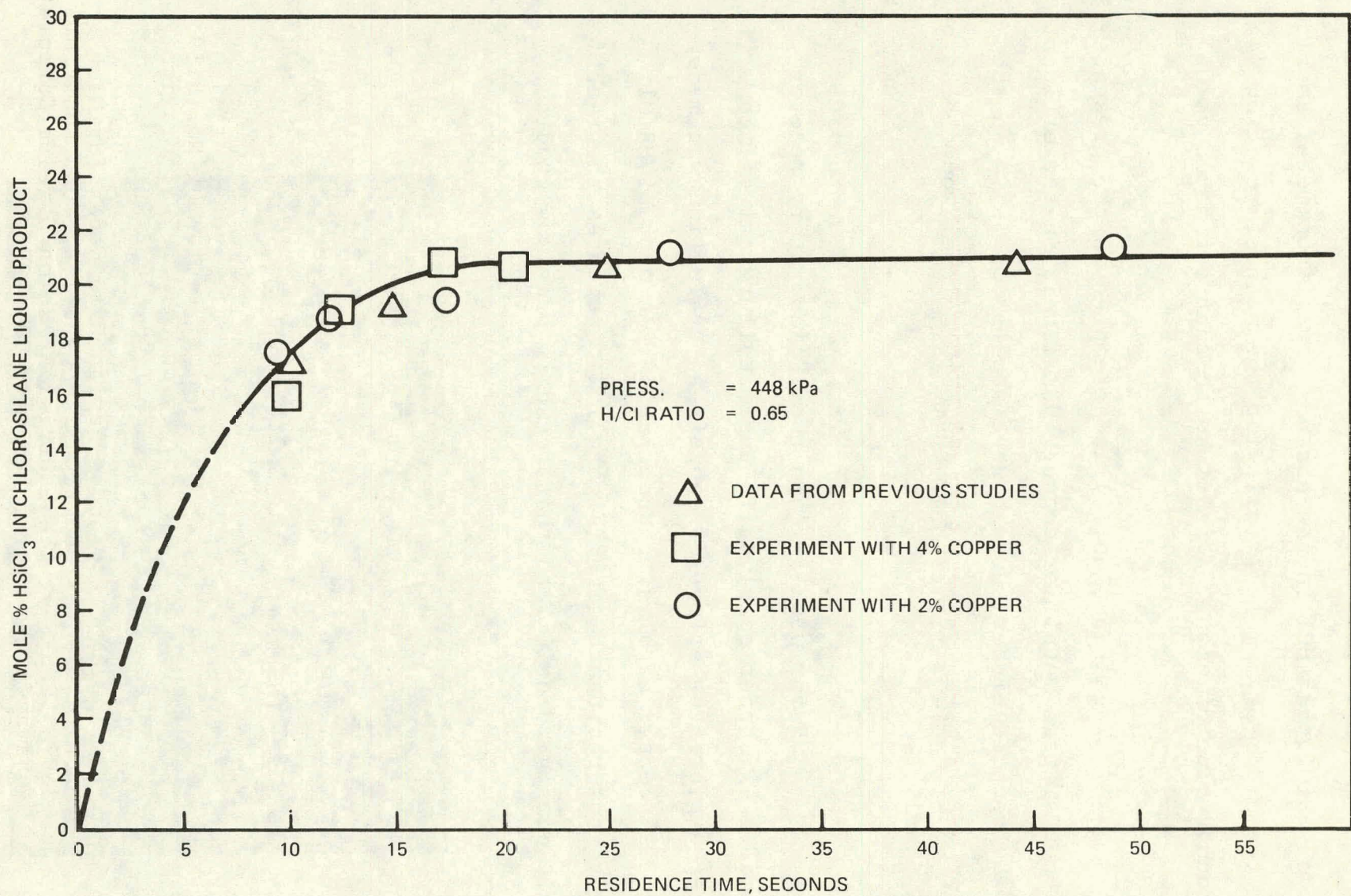


Figure 1.2
HYDROGENATION OF SiCl_4 TO HSiCl_3 AT 500°C

In a third set of experiments, the reactor was packed with copper-free metallurgical silicon. At 450°C to 500°C, the "uncatalyzed" yield of HSiCl_3 was found to be about 16% (Figures 1.3 and 1.4) at long residence time. That this value was substantially lower than when copper was also present (20%) is surprising. The difference between the "catalyzed" and "uncatalyzed" situations is larger as the reaction temperature is increased. Of the several possible explanations for this behavior (i.e., different relative ability of copper to absorb or desorb HCl or permanent change of the copper into a different state), the most critical from an operational view is the permanent change of the copper into a different, less active form.

Two samples of Cu/Si contact mass removed from reaction after 5.7% and 35% conversion of the silicon metal were analyzed microscopically. The scanning electron micrographs (SEM's) of both samples (Figure 1.5) showed pitting of the silicon metal surfaces. However, the attack was not uniform across the surface. Even after 35% conversion there were still areas seemingly untouched by the reaction. Both X-ray spot probe (E DAX) analysis and X-ray mapping of the surface confirmed that wherever the silicon surface was consumed, (pitted area), copper was invariably present. No copper was detected on the smooth original solid surfaces not evidently taking part in the reaction. The manner by which the silicon metal is consumed in this hydrogenation reaction might be described as a

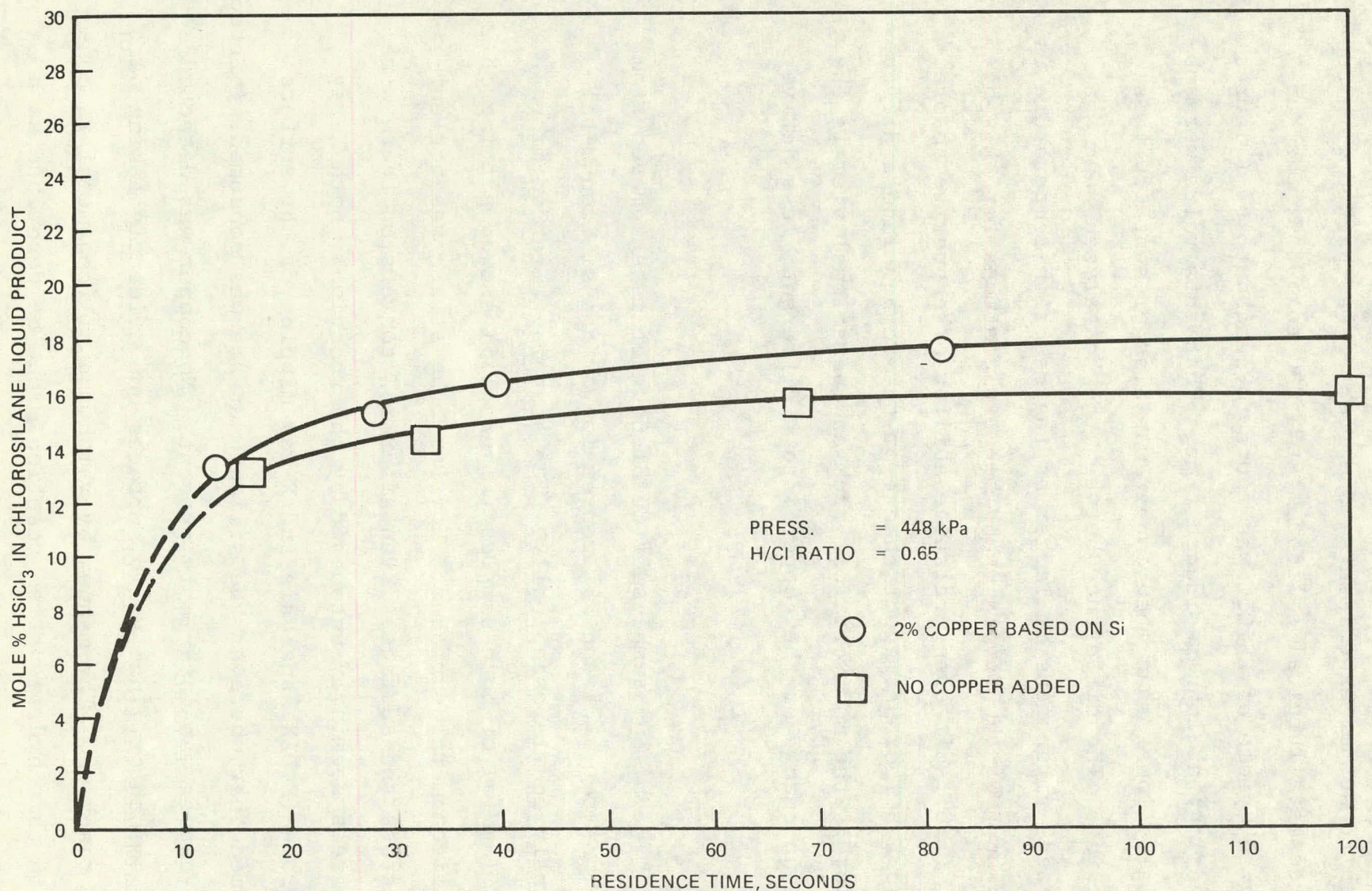


Figure 1.3
 HYDROGENATION OF SiCl_4 TO HSiCl_3
 AT 450°C , WITH AND WITHOUT COPPER CATALYST

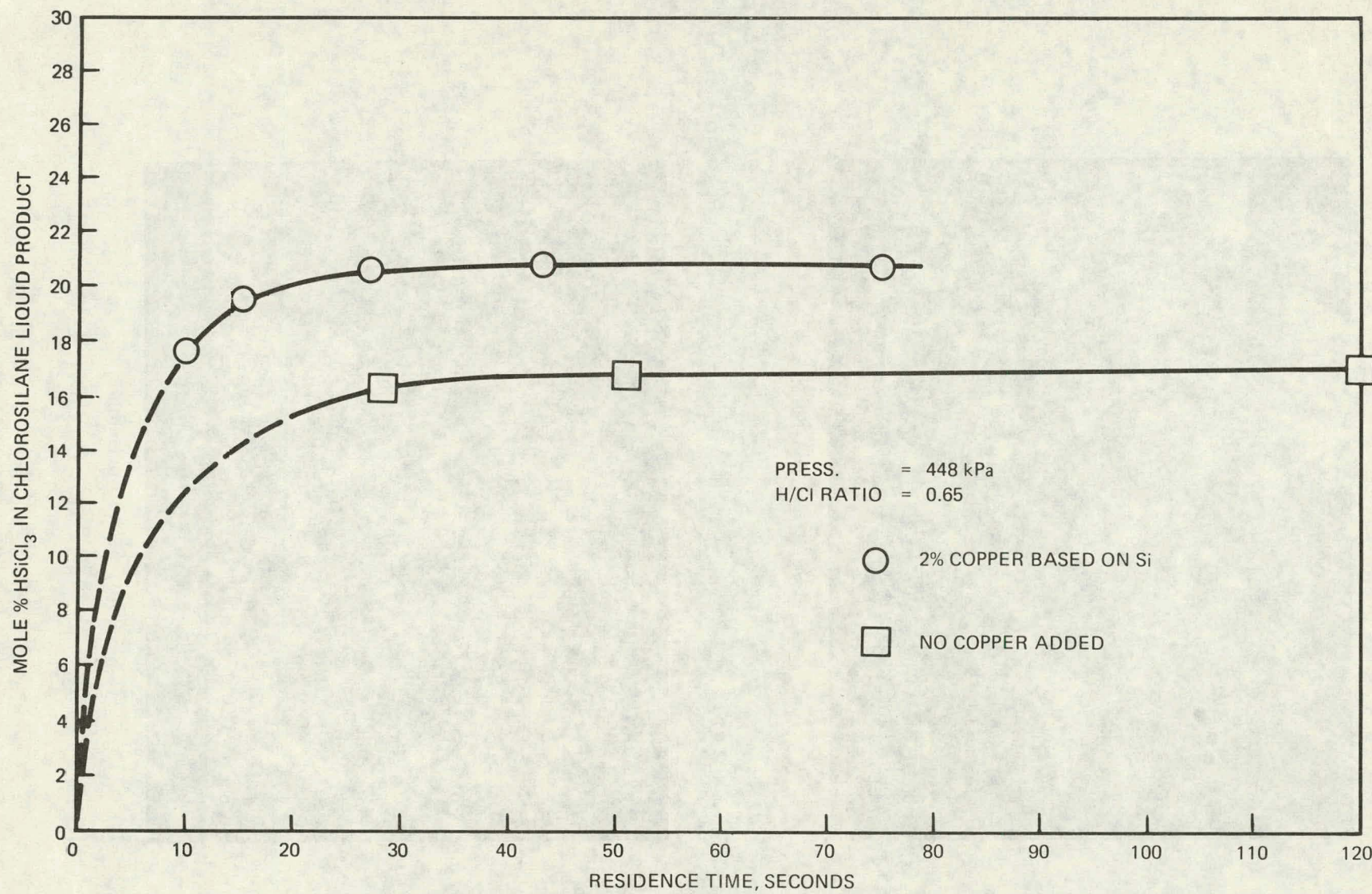


Figure 1.4
HYDROGENATION OF SiCl_4 TO HSiCl_3
AT 500°C , WITH AND WITHOUT COPPER CATALYST



(a) 35% Conversion



(b) 5.7% Conversion

Figure 1.5
SCANNING ELECTRON MICROGRAPHS
OF REACTED Cu/Si CONTACT MASS

"localized infection" which starts when a particle of copper becomes attached to silicon. Erosion of the silicon metal surface begins at that point and then spreads downward and outward as the reaction ensues. Photomicrographs of the silicon metal surface combined with X-ray maps show uniform distribution of copper at these craters. The original copper particles (mean diameter 9 microns) have completely disappeared. The SEM analyses show that the amount of copper present in the "infected" areas is but a small fraction of the total present in the bulk material. This supports the experimental findings that 50% reduction in copper usage did not alter the kinetic profile and further supports the rather high activity found in the 3" I.D. development reactor which had but 0.19% copper/silicon alloy.

1.2.2 THERMODYNAMIC ANALYSIS of the H-Si-Cl SYSTEM

The process route to low cost silane involves two types of equilibrium reactions. The hydrogenation of silicon tetrachloride in the presence of metallurgical silicon at circa 500°C provides the trichlorosilane for the subsequent disproportionation reactions forming ultimately silane and silicon tetrachloride. In the design of large scale process equipment, it is essential that the bulk heat effects be known. The published values of heats of formation of the silane compounds of interest result in calculated heat effects which do not agree with the more recent experimental findings. An analysis has been made to aid in resolving the discrepancies and provide meaningful design information.

The approach used to define the various heats of formation values was to use the variation of the equilibrium chemical composition with temperature to determine the heat of reaction and then using as a basis the heat of formation of silicon tetrachloride (which is quite well known and precise) to then calculate the heats of formation of the other chlorosilane compounds. Then using those values, the heat of reaction for all other equilibrium reactions involving the hydrochlorosilanes could be readily calculated.

The heat of reaction for the disproportionation of hydrochlorosilanes was calculated from the equilibrium data at various temperatures. Comparison of the calculated values with the experimentally observed heat effects indicates substantial agreement in that the reactions are essentially thermo-neutral. Values of heats of formation for dichlorosilane, derived from experimental data, show close agreement with published data in the JANAF Thermochemical Tables and the experimental value for trichlorosilane agrees with the recent data by Hunt^(1.0). (Figure 1.6)

While the found value for monochlorosilane is different from the published value, the experimentally determined value appears to be more consistent with observed heat effects and better fits the overall trend in the homologous series of chlorosilanes.

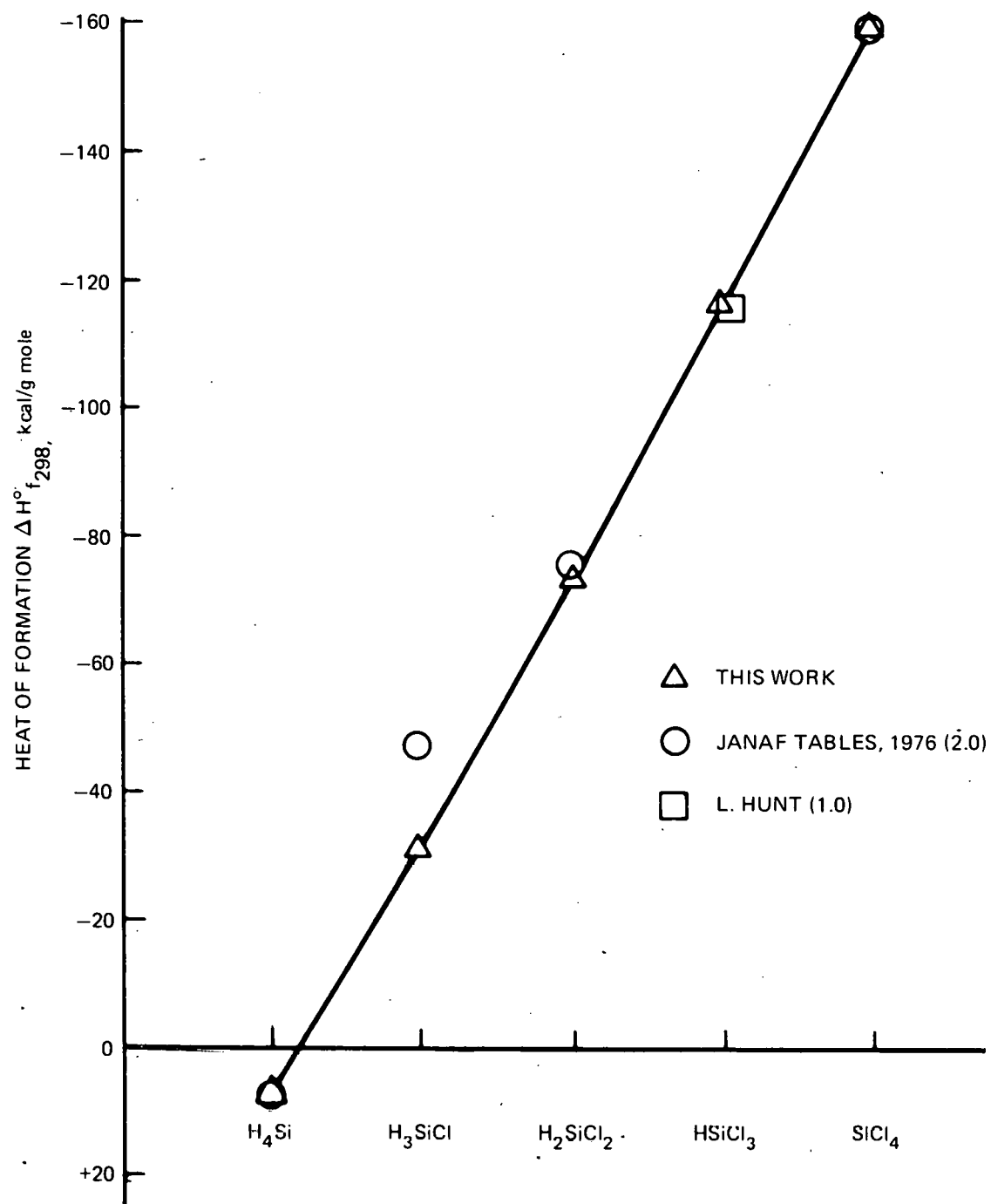


Figure 1.6
HEATS OF FORMATION OF HYDROCHLOROSILANES

The net heat effect in the disproportionation of tri- and dichlorosilanes is small. Although the calculated values indicate a potential of 2° and 50°C rise in temperature, respectively, small errors in either the equilibrium composition or in the heats of formation could result in the thermoneutral system which is experimentally observed.

1.2.3 INTEGRATED PROCESS OPERATION

Integration of the HSiCl_3 disproportionation reactor and distillation column with the hydrogenation and silane units has been accomplished. Using the silane still distillate and $\text{HSiCl}_3/\text{SiCl}_4$ crude from the hydrogenation unit as the only feed materials, the HSiCl_3 unit operated smoothly, producing $\text{H}_2\text{SiCl}_2/\text{HSiCl}_3$ feed for the silane unit, and recycle SiCl_4 for hydrogenation. Typical operating conditions for the operation are given in Figure 1.7.

Results of boron analysis for the trichlorosilane reactor inlet and outlet and of the still overhead are given in Table 1.2. While remaining constant through the reactor, most of the boron appears to be leaving the in the bottom stream of the trichlorosilane still. This result is unexpected because the anticipated boron compounds BCl_3 and B_2H_6 would exit in the overhead stream. It is possible that some of the boron at this point is in a heavier, complexed form. While due in part to some amount of highly pure start-up HSiCl_3 and SiCl_4

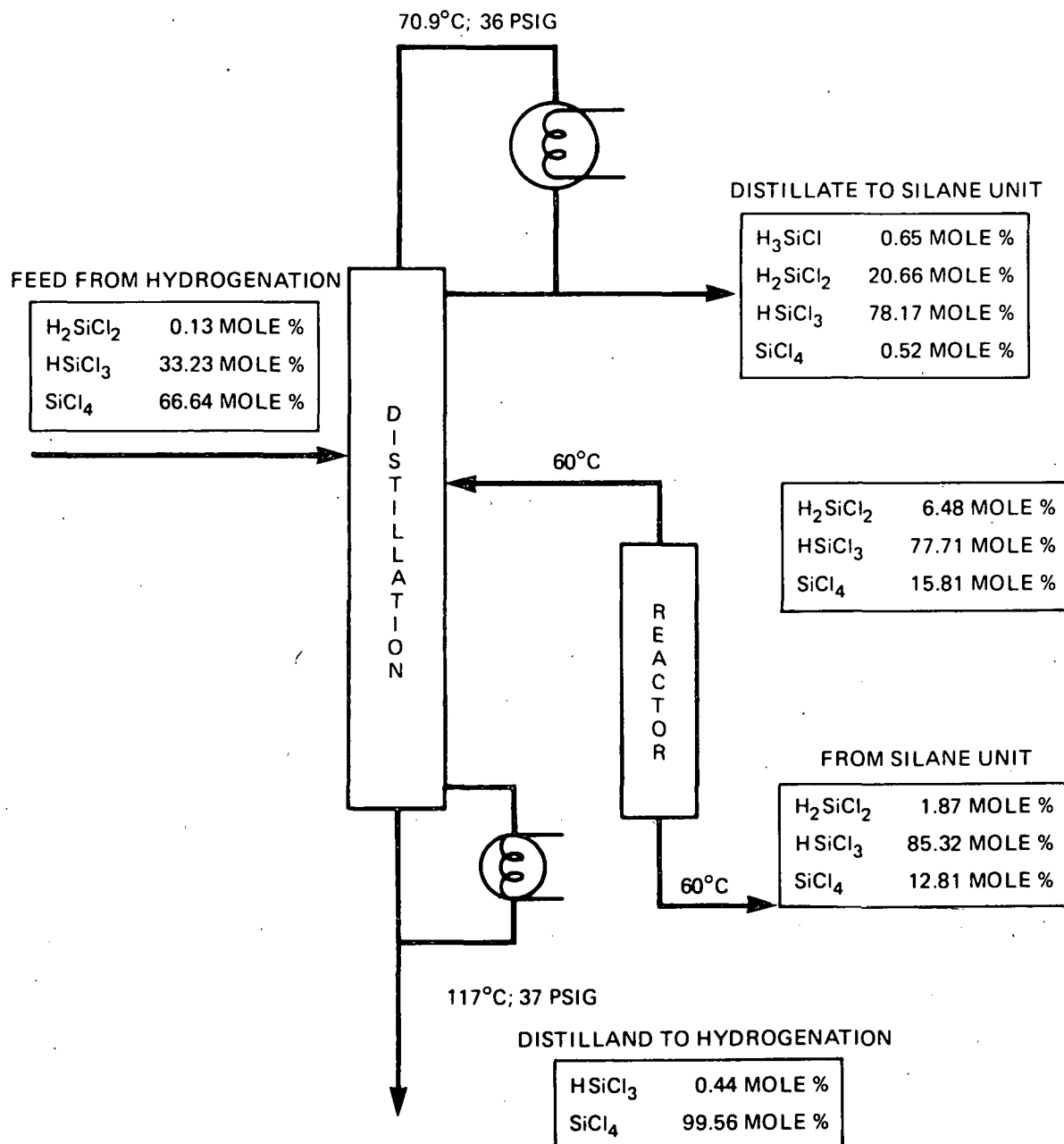


Figure 1.7
 HSiCl_3 DISPROPORTIONATION UNIT

remaining in the system, these extremely low boron levels are certainly well below the acceptable range for this part of the system. Analysis, which is currently under way, of the distill- and for boron could help to further define the material balance around the trichlorosilane still.

Table 1.2

BORON ANALYSIS AROUND HSiCl₃ UNIT

Stream	Parts per Billion Boron by Weight
HSiCl ₃ reactor inlet	0.13
HSiCl ₃ reactor outlet	0.12
HSiCl ₃ still overhead	0.04

The silane reactor and still were started up and operated using as feed material H₂SiCl₂/HSiCl₃ distillate from the trichlorosilane still. Several mechanical difficulties dealing with liquid gravity flow were identified and minor piping changes to correct them are currently being completed. This unit should be ready to operate routinely when the demonstration of the PDU integrated operation is finished next quarter. Silane made during that period will be compressed and stored in cylinders.

1.3 CONCLUSIONS

- Studies on the hydrogenation of silicon tetrachloride have shown the reaction to be mildly endothermic, its

kinetics to be a weak function of copper catalyst concentration, and its equilibrium to shift in the absence or presence of silicon and/or copper.

- Copper chloride and hydrogen chloride are likely intermediates in the hydrogenation reaction.
- A thermodynamic analysis indicates that thermal effects in the disproportionation reactions are minor.
- Data obtained to date in the process development unit indicate a close agreement between the design predictions and the operating results.
- The demonstration of the integrated operation of the process development unit is nearing completion and should be accomplished early next quarter.

1.4 PROJECTED QUARTERLY ACTIVITIES

- Complete the demonstration of the integrated operation of the Process Development Unit.
- Obtain more fluid-bed hydrogenation data at 500°C, the temperature being used in scale-up design.
- Begin additional hydrogenation studies with respect to the optimum catalyst loading, high pressure operation, and reaction pathway.

- Begin kinetic and equilibrium measurements for liquid phase redistribution of dichlorosilane at 80°C and 700 psig.
- Begin evaluation of means of improving the collection efficiency of impurities from the hydrogenation reactor.

1.5 REFERENCES

- 1.0 L. P. Hunt, E. Sirtl, D. H. Sawyer, J. Electro-Soc., 1974, 121 (7), 919-24.
- 2.0 D. R. Stull, A. Prophet, JANAF Thermodynamic Tables, Second Edition, V. S. Dept. of Commerce NBS, July 1977
- 3.0 W. C. Breneman, H. Cheung, E. G. Farrier, H. Morihara, Quarterly Progress Report, DOE/JPL 954334-7815

2.0 SILICON PRODUCTION

2.1 INTRODUCTION

The objective of this program, which started in January 1977, is to establish the viability and economic feasibility of manufacturing semiconductor-grade polycrystalline silicon through the pyrolysis of silane. The silane-to-silicon conversion is to be investigated in a fluid bed reactor and a free space reactor.

In the previous quarter, it was reported that a quartz fluid bed reactor was designed and constructed. This reactor was operated at temperatures up to 1000°C and silane was decomposed in it. The most practical method of producing seed material for the fluid bed reactor, from bulk silicon, was found to be comminution using a combined hammer mill-roller crusher system. In one free space reactor experiment, a silane-to-silicon conversion rate of 2.8 kg/hr was maintained for one hour. No measurable impurities were detected in a cathode layer emission spectroscopic analysis of free space reactor powder. A total impurity concentration of 2 μ g/g was detected after subjecting the powder to a chemical impurity concentration technique. A cast pellet of this powder had an electrical resistivity of 35-45 ohm-cm and a P-type conductivity. A melt consolidation apparatus was connected to the free space reactor to complete the in-line powder production, transfer, and melting system. A powder melting rate of 0.8 kg/hr was

obtained; polycrystalline rods suction-cast from this melt had P-type conductivities and an average electrical resistivity of 35 ohm-cm.

2.2 DISCUSSION

2.2.1 SILANE PYROLYSIS

2.2.1a FLUID BED REACTOR

The first silane-to-silicon conversion in the quartz fluid bed reactor was reported in the previous quarterly report. The bed of -35/+60 mesh silicon particles was fluidized with 50 ℓ/min of helium fed through the porous metal plate; simultaneously, a mixture of helium and silane was injected through the central spout orifice. The helium flow rate through the spout orifice was held constant at 30 ℓ/min while the silane flow rate was varied from 1 to 5 ℓ/min . The reactor wall temperature was maintained at 880°C to 890°C. During the current period, the products of that experiment were examined. Approximately 33% of the silicon produced was recovered as a loose powder. Figure 2.1 is a photomicrograph of cross sections of the coated seed bed particles; the coatings were porous and coatings up to 60 μm in thickness were measured. Approximately 60% of the particles that were microscopically examined had coatings.

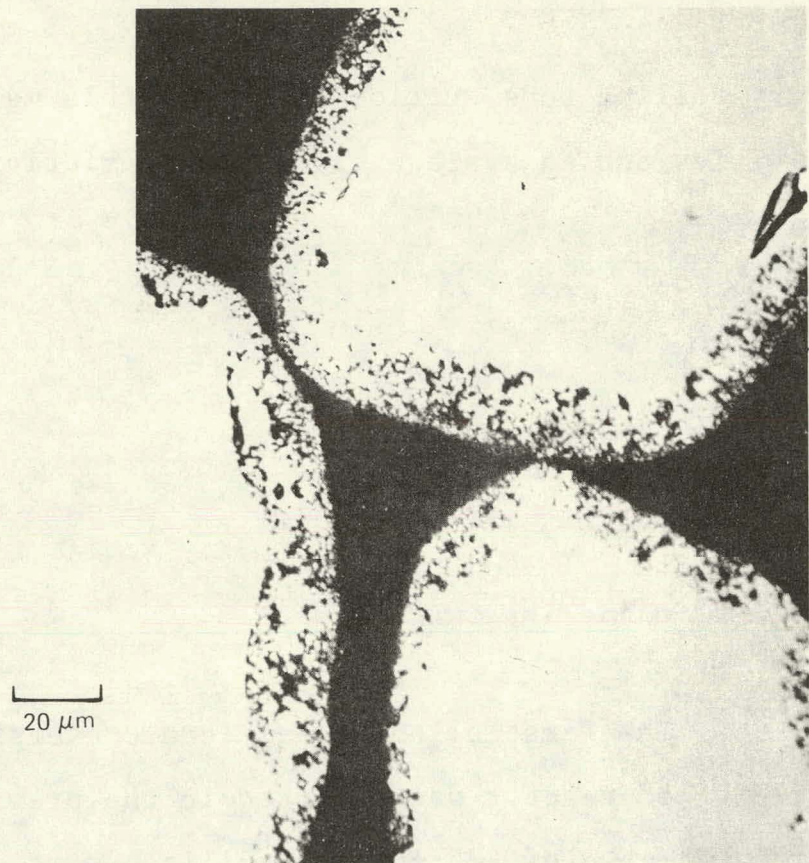


Figure 2.1
PHOTOMICROGRAPH OF CROSS-SECTIONED PARTICLES
COATED IN THE FLUID BED REACTOR

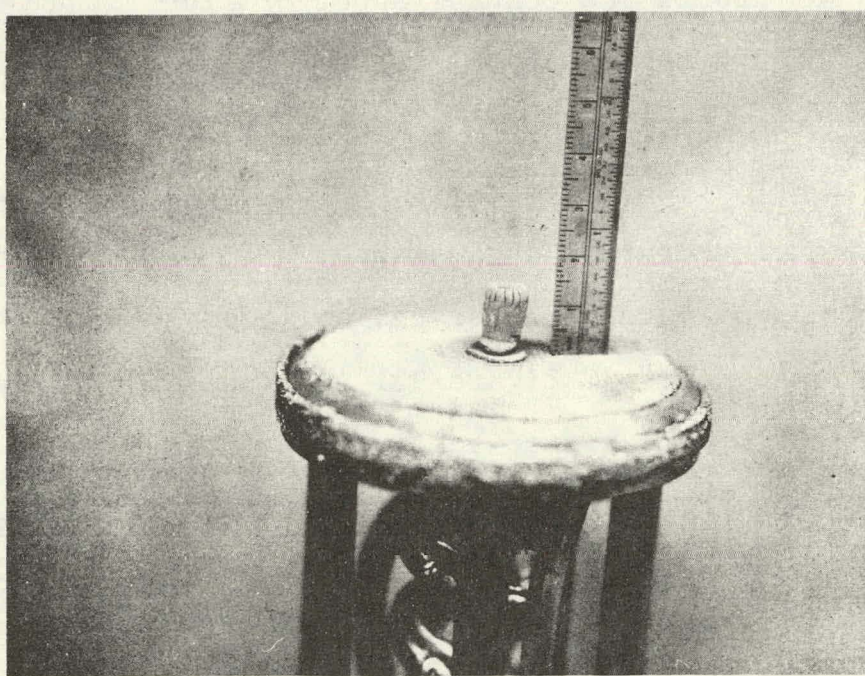


Figure 2.2
SILICON GROWTH OF FLUID BED REACTOR
GAS-INJECTION SYSTEM

During the current report period, additional silane pyrolysis experiments were conducted in the reactor containing the centrally located spout orifice. The experimental objectives were twofold. One objective was to ascertain whether or not the apparatus temperature and gas flow control systems were capable of maintaining a stable fluidized bed during prolonged experiments. The second objective was to identify potential problem areas; e.g., wall or gas injector reactions and factors contributing towards bed instability. In all elevated temperature experiments, the bed behavior was violent with particles ejected to 300 mm or more above the bed. Attempts at establishing a well-defined spout emanating from a fluidized bed were not successful. Difficulties were also experienced with the temperature control. Sufficient power was available, but the response time when changes did occur was slow. The fluid bed reactor was subsequently modified for more precise control of the bed temperature and particle behavior. The major modification was the elimination of the centrally located spout. A water-cooled porous metal (average pore size of 35 μm) gas distribution system was provided.

In the current series of experiments in which the spout orifice was used, difficulties were experienced in obtaining a mass balance. However, for experiments conducted at reactor temperatures ranging from approximately 850°C to 1000°C, the silicon product consisted of brown powder, a brown powdery-looking coating on the seed bed particles, and dense hollow silicon formations that grew around the central spout orifice (Figure 2.2). The mixture of silane and helium injected through the spout orifice contained 4.5% silane; helium was injected simultaneously through the fluidizer plate. By virtue of the construction of the gas injection system, the area surrounding the central orifice was solid metal. The growth occurred on this portion

of the injector system. The presence of this stagnant flow region or inadequate cooling of the gas injection system may account for the injector growth formations. In all experiments, good gas flow control was obtained. The silane-to-silicon conversion experiments were conducted for periods of up to two hours without reactor wall formations and without locking up the bed.

The range of gas velocities within which stable fluidized beds will occur at various operating temperatures will be established before additional silane pyrolysis experiments are conducted. The fluidization behavior of -35/+60 mesh silicon particles was determined, using the water-cooled porous metal gas distributor, for bed depths ranging from 50 mm to 200 mm and temperatures up to 950°C. The data for the onset of fluidization are in good agreement with the calculated minimum fluidization velocities.(2.5.1) The mathematical relationship, presented by Steward and Davidson^(2.5.2) for predicting the room temperature transition from a fluidized to a slugging bed, did not agree with the experimental data. However, the elevated temperature data for this phase transition were in agreement with values calculated from the observed room temperature behavior and the volume expansion of the idealized fluidizing gas with increasing temperature. The calculations predicted that the range of gas velocities over which stable bed action was obtained decreased with increasing temperature. If subsequent experiments with different silicon particle size distributions and bed depths follow this pattern, then stable bed conditions may be predictable from room temperature observations.

2.2.1b FREE SPACE REACTOR

The free space reactor was operated for eight hours with 100% silane flowing continuously at a rate sufficient to produce 0.45 kg of silicon per hour. The

experiment was terminated as scheduled. The silane-to-silicon conversion efficiency was at least 94%. Post-inspection revealed that no semi-solid silicon formed on the reactor wall or on the gas injector.

An experimental lot (No. LK-289962) of silane^(2,5,3) was converted into silicon powder in the free space reactor. No difference in pyrolysis behavior was observed between the experimental lot of silane and the commercially available semi-conductor grade silane normally used in the current program. There was also no difference in product morphology. No impurities were detected when the powder was examined with an emission spectroscope using the cathode layer technique. When using the impurity concentration technique (described in the July-September, 1977, Quarterly Report), the impurity level appeared higher than recent runs made from commercially available silane. The sources of contamination have not been identified.

Thermodynamic calculations^(2.5.4) indicated that an adiabatic conversion of silane-to-silicon may occur at approximately 400°C in the free space reactor. The kinetic data^(2.5.5) indicated that the reaction rate at that temperature was too slow to support an efficient decomposition. An efficient silane-to-silicon conversion in the current reactor was not obtained when reactor wall temperatures were below approximately 800°C.

The efficient conversion of silane-to-silicon in the free space reactor was dependent upon the transfer of heat into the core of the injected silane stream. Several experiments were conducted to determine the minimum operating temperature for the complete conversion of silane-to-silicon at various silane flow rates. A constant silane

flow was maintained while the reactor temperature was varied. The color of the exhaust flame was monitored as an indication of the conversion efficiency. The data showed that, for the current reactor-injector configuration, a reactor wall temperature of at least 800°C was needed for complete conversion. When silane was injected into the free space reactor at a Reynolds Number below approximately 2000, a higher reactor temperature was needed to obtain complete conversion efficiency. A Reynolds Number greater than 2000 corresponds to a turbulent jet stream. Similarly, for Reynolds Numbers above 6000, the reactor temperature had to be gradually increased above the 800°C minimum to accommodate the higher gas velocities. The rate at which 50% of the silane present decomposes into silicon and hydrogen varies from approximately 0.5 seconds at 600°C to 1×10^{-5} seconds at 900°C.^(2.5.5) Consequently, small increases in temperature above the threshold value greatly increase the efficient production of silicon for a given reactor configuration.

In a series of experiments with the free space reactor, a qualitative correlation was made between the color of the exhaust flame and the silane-to-silicon conversion efficiency. When the outer fringe of the flame was white while the bulk of the flame was transparent or orange, the conversion efficiency was approximately 99%. When the entire flame was white, bordering on bright white, the conversion efficiency was approximately 97%. For lower efficiencies, the flame became too bright to observe directly.

A pneumatic powder transfer system was constructed and installed inside of the settling chamber of the free space reactor. This installation completed the in-line connection between the free space reactor and the melt consolidation apparatus. In the first performance evaluation test, all of the powder contained in the settling chamber was transferred to the hopper of the melt consolidator.

However, the powder transfer rate was not controllable nor continuous. It was found that smooth continuous transfer was dependent upon maintaining a pressure differential between the settling chamber and the elevated hopper. With the current gas inlet and exhaust system, this pressure differential could not be maintained. The engineering modifications needed to improve the current system will be implemented if the need arises. Continuous and controllable powder transfer rates are needed for the melting operation; consequently, the engineering studies associated with powder transfer will continue.

2.2.2 SILICON CONSOLIDATION

Two kilograms of free space reactor powder that had been pneumatically transferred to the hopper of the melt consolidator was continuously fed into a hot quartz crucible and melted. The quartz crucible was empty at the start of the experiment. In previous experiments, melting and powder feedrates were established after a molten pool of silicon was obtained in the crucible. The powder transfer rate to the crucible was 1.14 kg/hr. During this experiment, the powder melted as rapidly as it was transferred. This was the second experiment in which free space reactor silicon powder was produced, transferred, and melted in the enclosed in-line system. The molten silicon surface was dross free.

An attempt was made to establish the maximum rate at which free space reactor powder could be fed continuously into the 152 mm diameter quartz crucible of the melt consolidator and melted. During the first 15 minutes of the experiment, powder fed into the crucible at a rate of 1.56 kg/hr melted as rapidly as it was fed. During the next 15 minutes, a dross formed on the surface of the melt that reduced the

surface area of the exposed liquid silicon. Nevertheless, a steady powder feed and melting rate was maintained. A portion of the free space reactor powder used in this experiment had previously been handled and exposed to air. Previous work indicated that handling the powder could introduce sufficient impurities to cause dross formation. Additional experiments will establish the maximum feed and melting rate of free space reactor powder in the melt consolidation apparatus.

Vacuum-melted and cast pellets of both free space reactor powder and semi-conductor grade silicon were forwarded to JPL for purity analysis. A free space reactor powder sample was also sent with the cast pellets. The vacuum pellet-casting apparatus was previously described. Samplings of the powder were melted and cast into commercial and high purity grade^(25,6) quartz crucibles. The semi-conductor nuggets were melted and cast into commercial grade quartz. Table I lists the pertinent feedstock details and the electrical resistivity and conductivity type of the polycrystalline pellets. The resistivity was affected by the purity of the quartz melting crucible.

Table 2.1
PROPERTIES OF VACUUM MELTED AND CAST PELLETS

<u>Feedstock</u>	<u>Source</u>	<u>Quartz Crucible</u>	<u>Resistivity, ohm-cm</u>	<u>Conductivity Type</u>
Powder	Exp. #HPR-626-6-27	Commercial Grade	20	P
Powder	Exp. #HPR-626-6-27	High Purity	120	P
Nuggets	Dow	Commercial Grade	30	P

2.3 CONCLUSIONS

Experiments were conducted in a quartz fluid bed reactor to determine the conditions under which stable bed behavior could be obtained at room and elevated temperatures. Stable spout-fluidized beds were obtained at room temperature

for various seed bed conditions. However, at elevated temperatures, all attempts at establishing a well-defined spout projecting from a fluidized bed were unsuccessful. Preliminary experiments with the spout orifice removed showed that the range of gas velocities over which a stable fluidized bed was obtained decreased with increasing temperature. Additional experimental data are needed to determine if the stable bed conditions are predictable from room temperature observations.

It was demonstrated that the free space reactor could operate continuously for eight hours producing silicon powder at the rate of 0.45 kg/hr. This powder was pneumatically transferred to the hopper of the melt consolidation apparatus and subsequently melted at a rate of 1.14 kg/hr. A dross-free casting was obtained.

The electrical resistivity of cast silicon is affected by the purity of the quartz melting crucibles. Powder from one free space reactor experiment was melted and cast in both standard grade and high purity quartz crucibles. The polycrystalline electrical resistivities were 20 ohm-cm and 120 ohm-cm, respectively.

2.4 PROJECTED QUARTERLY ACTIVITIES

2.4.1 FLUID BED REACTOR

- Establish the range of gas velocities that will sustain a stable fluidized bed at elevated temperatures for various particle size distributions and bed depths.

- Inject mixtures of silane and helium into stable fluidized beds of silicon particles at various temperatures. Determine the nature of the silicon product, the efficiency of the silane-to-silicon conversion, and the elutriation rate.

2.4.2 FREE SPACE REACTOR

- Continue to identify factors for optimizing the pneumatic transfer of silicon powder.
- Generate engineering data for plant design and scale-up.
- Determine operating parameter effects on production rates.

2.4.3 SILICON CONSOLIDATION

- Optimize control of the rate of powder feed from the hopper to the furnace of the melt consolidation apparatus.
- Continue with experiments that will establish the optimum combined feed and melting rate of free space reactor powder in the melt consolidation apparatus.

2.5 REFERENCES

- 2.5.1 Kunii, D. and Levenspiel, O., "Fluidization Engineering," John Wiley & Sons, Inc., New York, 1969, pg. 73.
- 2.5.1 Steward, P. S. B. and Davidson, J. F., Powder Tech. 1, 61-80 1967.
- 2.5.3 Produced by Union Carbide Corporation under JPL Contract 954334.
- 2.5.4 Thermochemical data obtained from the JANAF Tables.
- 2.5.5 Hogness, T. R.; Wilson, T. L.; and Johnson, W. C.; American Chemical Society J., 58, 108-112, 1936

3.0 PROCESS DESIGN

3.1 INTRODUCTION

The purpose of this program, started in October 1977, is to provide JPL with engineering and economic parameters for an experimental facility capable of producing 25 metric tons of silicon per year by the pyrolysis of silane gas. An ancillary purpose is to estimate the cost of silicon produced by the same process on a scale of 1000 metric tons per year.

Key equipment such as the hydrogenation reactor, redistribution reactors, distillation columns, adsorption beds, and pyrolysis/melting system was designed for the 25 MT/yr experimental facility. A preliminary process design package was subsequently prepared and is undergoing a final inspection.

A scale model of a 1000 MT/yr plant was built and used in generating a detailed plant cost. The product cost analysis shows that the product selling prices will be substantially less than the DOE/JPL 1986 cost goal of \$10/kg. The plant costs for 25, 50, and 100 MT/yr capacities were computed by scaling the 1000 MT/yr plant estimate. It appears that the product selling price from the 100 MT/yr plant will meet the JPL/DOE 1982 intermediate cost goal of \$25/kg.

Before the process design of the 25 MT/yr experimental facility can be finalized, some process design data

need to be generated experimentally. Arrangements have been completed to start acquisition of these data in-house. All necessary data should be available by September 1978.

3.2 DISCUSSION

3.2.1 PROCESS SPECIFICATIONS UPDATE

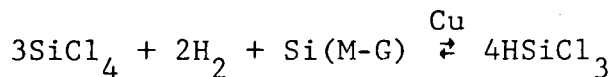
Preliminary process specifications established earlier (3.1, 3.2) have been updated and all current process design efforts are based on these updated specifications.

Plant Capacity. The experimental facility produce 25 MT/yr of semiconductor-grade silicon and it is assumed that it will be on-stream 63% of the year. The following flow rates will be used:

Metallurgical-Grade Silicon	12.0 lb/hr
Hydrogen to Hydrogenation Reactor	1.5 lb/hr
Silicon Tetrachloride Make-up to Hydrogenation Reactor	13.3 lb/hr
Silane to Pyrolysis Reactor	12.0 lb/hr
High-Purity Silicon Product	10.0 lb/hr
Hydrogen Effluent from Pyrolysis Reactor	1.5 lb/hr
Silicon Powder Loss	0.5 lb/hr

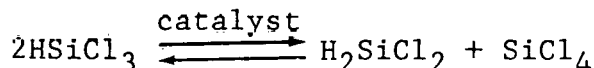
Hydrogenation. Hydrogenation of silicon tetrachloride (STC) is carried out in a fluid bed reactor and is

represented by the following equation:



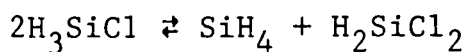
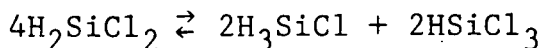
Hydrogenation Reactor	fluid bed
Temperature	500°C
Pressure	500 psig
Mean Particle Diameter of Silicon	150 μm
Fluidization Velocity	0.25 ft/sec
Gas Residence Time in Bed	20 seconds
Catalyst	Copper
Catalyst/Si(M-G) Feed Ratio	3 to 4%

Trichlorosilane Redistribution. The redistribution of TCS into dichlorosilane and STC is effected in the presence of an ion exchange catalyst. The reaction is represented by:

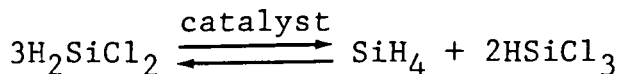


Redistribution Reactor	packed bed
Temperature	70°C
Pressure	85 psia
Fluid State	liquid
Residence Time	10 minutes
Catalyst	Amberlyst A-21 resin

Dichlorosilane Redistribution. The redistribution of dichlorosilane to produce silane and TCS is carried out over the amine catalyst according to the following equations:



The net reaction is:



Redistribution Reactor	packed bed
Temperature	50°C
Pressure	550 psia
Fluid State	liquid
Residence Time	42 minutes
Catalyst	Amberlyst A-21 resin

Silane Purity. In order to attain the desired purity for the silicon product, silane fed to the pyrolysis reactor must meet the following requirements:

	<u>Required</u>	<u>Expected Max. Level from UCC Process</u>
Phosphorus	1 ppb	0.15 ppb
Boron	0.3 ppb	0.06 ppb
Iron, heavy metals	1 ppb	1 ppb
Carbon	5 ppb	1 ppb
Chlorosilanes	20 ppm	1 ppb
Nitrogen	500 ppm	1 ppm
Hydrogen	1%	1 ppm
Moisture	-80°C dew point	1 ppm

3.2.2 KEY EQUIPMENT DESIGN for the 25 MT/yr FACILITY

3.2.2a HYDROGENATION

A preliminary conceptual design of a fluidized-bed reactor was completed and documented^(3.3) for the hydrogenation of silicon tetrachloride in the presence of metallurgical-grade silicon. The reactor product contains trichlorosilane which is used in the synthesis of high-purity silane by disproportionation and distillation. The hydrogenation reaction is carried out at 500°C and 500 psig using a copper catalyst which effects near-equilibrium conversion within a few seconds.

Analysis of fluidization parameters suggests that the reactor for a 25 MT/yr plant should be operated with silicon particles having a mean diameter of 150 microns fluidized at a superficial gas velocity of 0.25 ft/second. The reactor size is 8" nominal diameter with an expanded freeboard section of 14" diameter. The recommended mean particle diameter for the 1000 MT/yr plant hydrogenation reactor is 250 microns. The fluidization velocity for this case should be about 0.5 ft/second in a reactor 2.5 ft in diameter with the freeboard expanded to a diameter of 6.5 ft.

3.2.2b REDISTRIBUTION

Available experimental data for redistribution of trichlorosilane over Rohm and Haas Amberlyst A-21 catalyst has been fitted to kinetic expressions.^(3.4) At high temperatures, both liquid and vapor phase reactions are diffusion controlled and exhibit first-order behavior. At lower

4

temperatures, second-order behavior prevails. The reactions exhibit Arrhenius temperature dependence of the reaction-rate constant. Sufficient information is provided to size both liquid- and vapor-phase, fixed-bed reactors. It now appears that any future trichlorosilane redistribution will occur in a liquid-phase reactor operating at 85 psia. The expected moderate operating pressures prevent consideration of vapor-phase operation because of temperature/vapor pressure constraints. Certain additional experimental data are needed to resolve observed variations in catalyst activity and to define liquid-phase equilibrium and kinetic performance of the catalyst, particularly in the 60° to 80°C temperature regime.

3.2.2c DISTILLATION

As shown in Figure 3.1, all four distillation columns for the 25 MT/yr experimental facility have been designed. The design is still preliminary since experimental thermodynamic data such as vapor/liquid equilibrium of certain chlorosilanes will not be available for another two or three months. Process designs will be reviewed and adjusted as required when accurate data become available.

The first column (D-1) in Figure 3.1 is the stripper where all trace light gases are removed as the overhead vapor product. The light key is hydrogen chloride which must be removed if present. The heavy key is dichlorosilane. The column

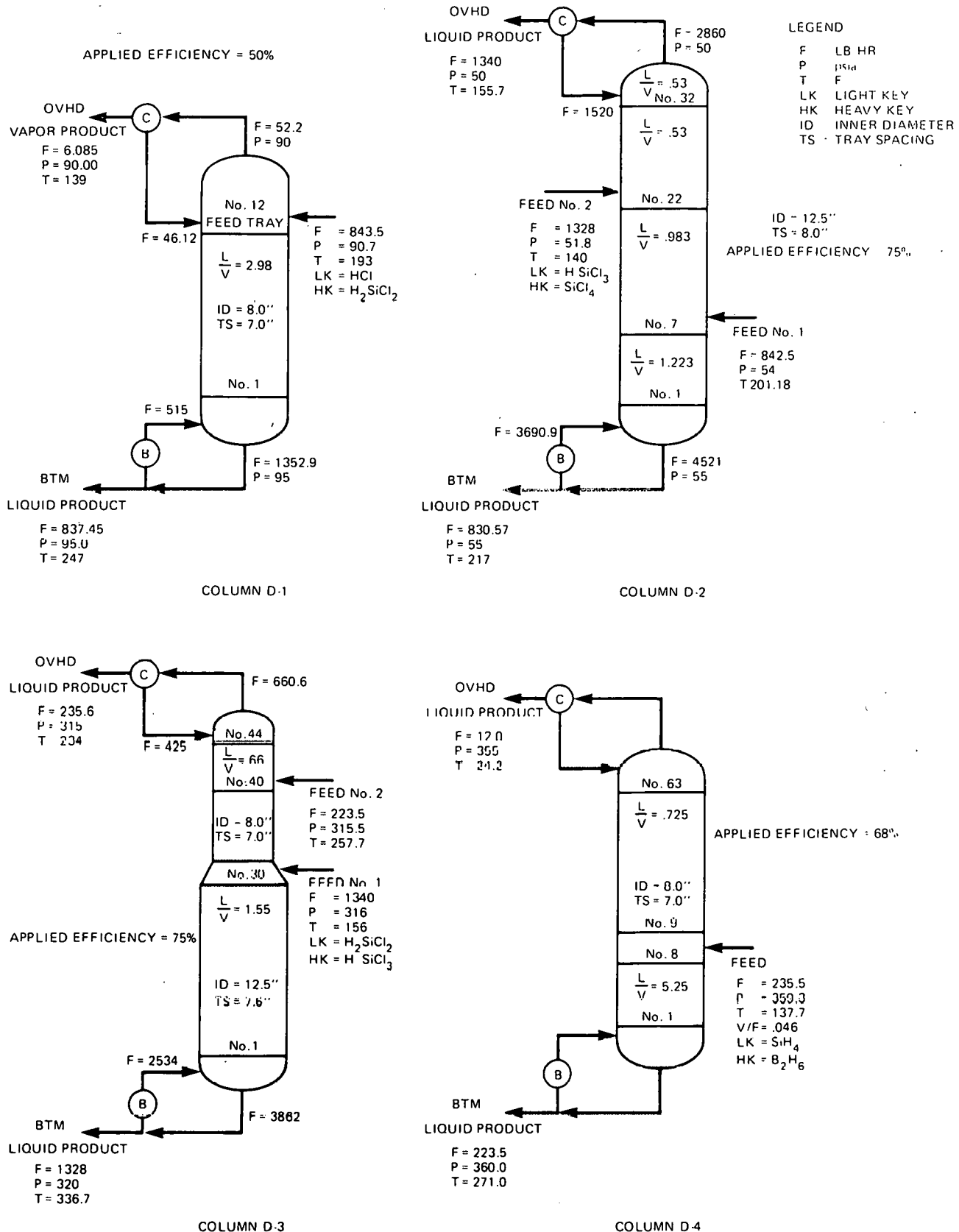


Figure 3.1
DISTILLATION COLUMN DESIGN FOR THE 25 MT/Y EXPERIMENTAL FACILITY

has 12 trays and the applied efficiency is 50 percent. The second column (D-2) separates trichlorosilane from silicon tetrachloride at 50 psia. There are 32 trays and the applied efficiency is 75 percent. The third column (D-3) has two diameters to accommodate its flow variations. The first 30 trays have a diameter of 12.5 inches and the top 14 trays have a diameter of 8 inches. This column separates TCS from DCS. It operates at 315 psia and the applied efficiency is 75 percent. The last column (D-4) is the silane distillation column where an ultra-pure silane is taken out as the overhead liquid product and all chlorosilanes are removed as a bottom product. This column operates at 360 psia and the applied efficiency is 68 percent.

3.2.2d ADSORPTION

Although the silane distillation column is designed to produce silane having one part-per-billion-level impurities, an activated carbon trap will be installed to guard against an unexpected upset condition.(3.5) We assumed that in an upset condition, there are 2.46 mole % MCS and 0.56 mole % DCS in the silane stream.

To allow for continuous operation, the adsorption system consists of two vessels containing activated carbon. One is on an adsorption cycle while the other is on a reactivation cycle. The cycle time is eight hours.

3.2.2e PYROLYSIS/MELTING

A conceptual design of the free-space reactor and powder consolidation for a 25 MT/yr plant is complete. The cross-sectional view of the pyrolysis/melter system is presented in Figure 3.2, and the parts list is given in Table 3.1. In this scheme, the ultra-pure silicon powder produced in the free-space reactor falls to the storage hopper from where it is transferred into one of two melters, the other one being a spare. Polycrystalline silicon rods could be pulled from the top of the melter.

Heat balance calculations around the pyrolysis reactor and melter show that a net heat input of approximately 3.0 KW/kg of silicon is required. An induction heating furnace of 15 KW is recommended.

For the 1000 MT/yr plant, we will probably need three half-size free-space reactors, one of which is a spare. The reactor diameter will be about 3 ft. Six melters need to be provided, one of which is a spare.

This design was reviewed by our in-house consultants and some valuable comments were received. A departmental engineering memorandum is being prepared to document the pyrolysis reactor/melter design. It lists the assumptions

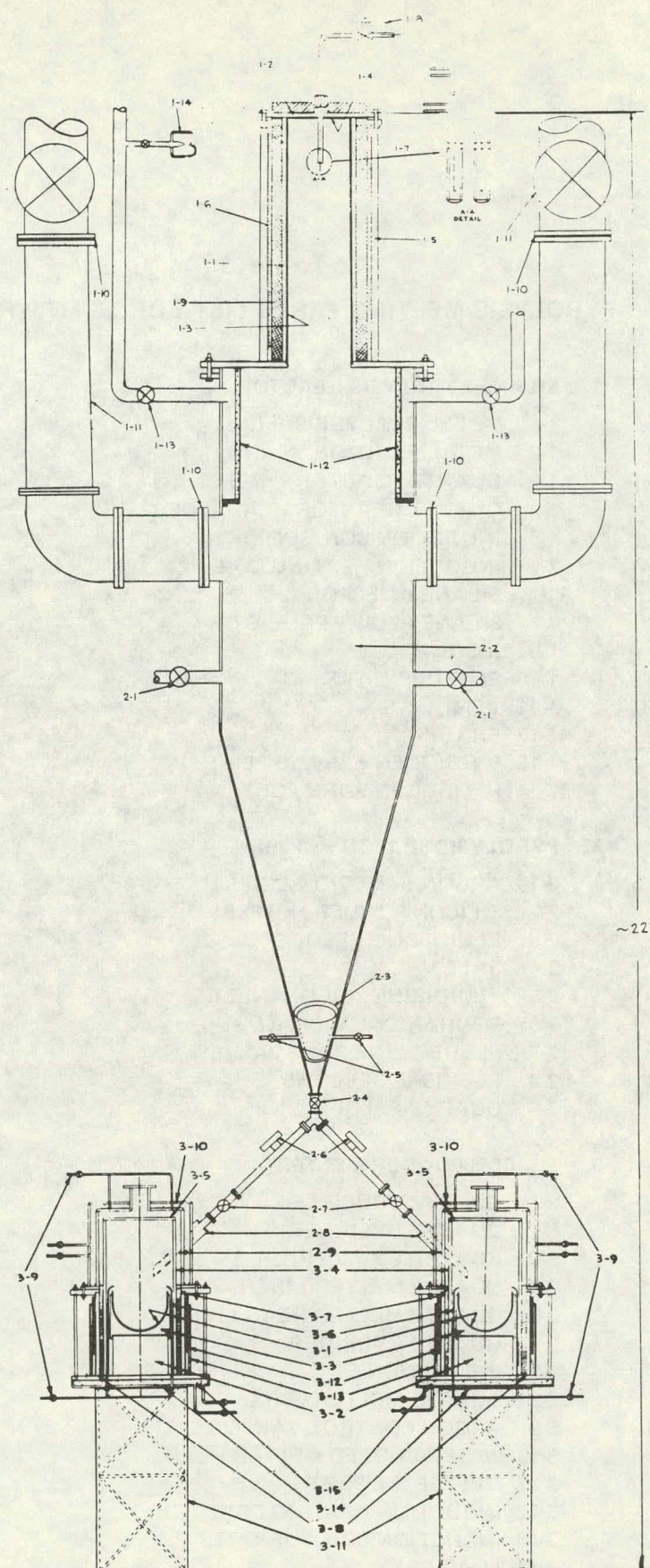


Figure 3.2

25 MT/yr EXPERIMENTAL FACILITY
SILANE PYROLYSIS & POWDER MELTING APPARATUS

Table 3.1
PYROLYSIS/MELTING PARTS LIST FOR 25 MT/YR PLANT

- 1. SILANE PYROLYSIS REACTOR**
 - 1-1 METAL REACTOR SHELL
 - 1-2 METAL REACTOR HEAD
 - 1-3 QUARTZ REACTOR LINER
 - 1-4 QUARTZ REACTOR HEAD LINER
 - 1-5 INDUCTION COIL SUPPORTS
 - 1-6 INDUCTION HEATING COIL
 - 1-7 SILANE INJECTOR
 - 1-8 SILANE FLOW REGULATOR
 - 1-9 INSULATION
 - 1-10 RUPTURE DISKS
 - 1-11 VENT LINE
 - 1-12 FILTER
 - 1-13 HYDROGEN EXHAUST LINE
 - 1-14 HYDROGEN BURN PORT
- 2. PYROLYSIS SILICON HOPPER**
 - 2-1 ARGON INJECTION LINES
 - 2-2 SILICON POWDER HOPPER
 - 2-3 FLUIDIZING FEEDER
 - 2-4 BALL VALVE
 - 2-5 FLUIDIZING ARGON INLET
 - 2-6 MECHANICAL VIBRATORS
 - 2-7 FEEDER INLET VALVES
 - 2-8 FLEXIBLE BELLOWS
 - 2-9 QUARTZ FEEDER LINES
- 3. SILICON POWDER MELTER**
 - 3-1 QUARTZ CRUCIBLE
 - 3-2 QUARTZ CYLINDER
 - 3-3 GRAPHITE SUSCEPTOR
 - 3-4 QUARTZ MELTER LINER
 - 3-5 QUARTZ MELTER HEAD LINER
 - 3-6 QUARTZ CYLINDER
 - 3-7 INSULATION
 - 3-8 QUARTZ MELTER WALL
 - 3-9 ARGON CONTROL VALVES
 - 3-10 WATER COOLED MELTER HEAD
 - 3-11 MELTER SUPPORT
 - 3-12 INDUCTION HEATING COIL
 - 3-13 INDUCTION COIL SUPPORTS
 - 3-14 LOAD CELL
 - 3-15 MELTER BOTTOM PLATE

and uncertainties associated with the present design and also includes recommendations for some developmental programs which take into account the consultant's comments.

3.2.3 SGS PROCESS DESIGN PACKAGE for the 25 MT/YR FACILITY

We recently completed assembly of a preliminary SGS (semiconductor-grade silane/silicon) process design package for the 25 MT/yr experimental facility. The package consists of the following:

Detailed Process Description. The description written as a departmental engineering memorandum, (3.6) is divided into four sections - Hydrogenation, Distillation/Redistribution, Silane Pyrolysis/Consolidation, and Waste Disposal.

Equipment Data Sheets. All 60 pieces of major equipment were identified and specifications prepared. The equipment was divided into ten classes; thus, ten separate specification forms are being used. They are: B - Bins, C = Compressors, D - Distillation Columns, F - Filters, H - Heat Exchangers, P - Pumps, R - Reactors, S - Solid Handling Equipment, T - Tank, and U - Others (Ejector, Agitator, and Furnace).

Heat and Mass Balance - The balance is in the form of a computer output and only major streams are listed. Trace impurities are not included.

Process Flow Diagram. The diagram consists of four sheets; one each for the Hydrogenation, Distillation/Redistribution, Pyrolysis/Consolidation, and the Waste Disposal Sections,

Layout Drawing. The layout for the 25 MT/yr plant was scaled down from the 1000 MT/yr plant.

Electric One-Line Drawing

Pyrolysis Unit Drawing. The pyrolysis/melter system is unconventional. For this reason, an assembly drawing of the overall system was included in the process design package.

3.2.4 SGS PROCESS DESIGN for a 1000 MT/YR COMMERCIAL PLANT

3.2.4a PROCESS FLOW DIAGRAM

As stated in the last quarterly progress report, two silane production schemes have been under consideration: the Adsorption Silane Process and the Distillation Silane Process. In early January, the two process schemes were critically reviewed resulting in a hybrid purification scheme shown in Figure 3.3. In this scheme, the distillate from the third column, containing di- and monochlorosilanes, is fed to a redistribution reactor and ultra-high purity silane is separated from the redistribution products by distillation in a final column. This arrangement requires fewer pieces of equipment than

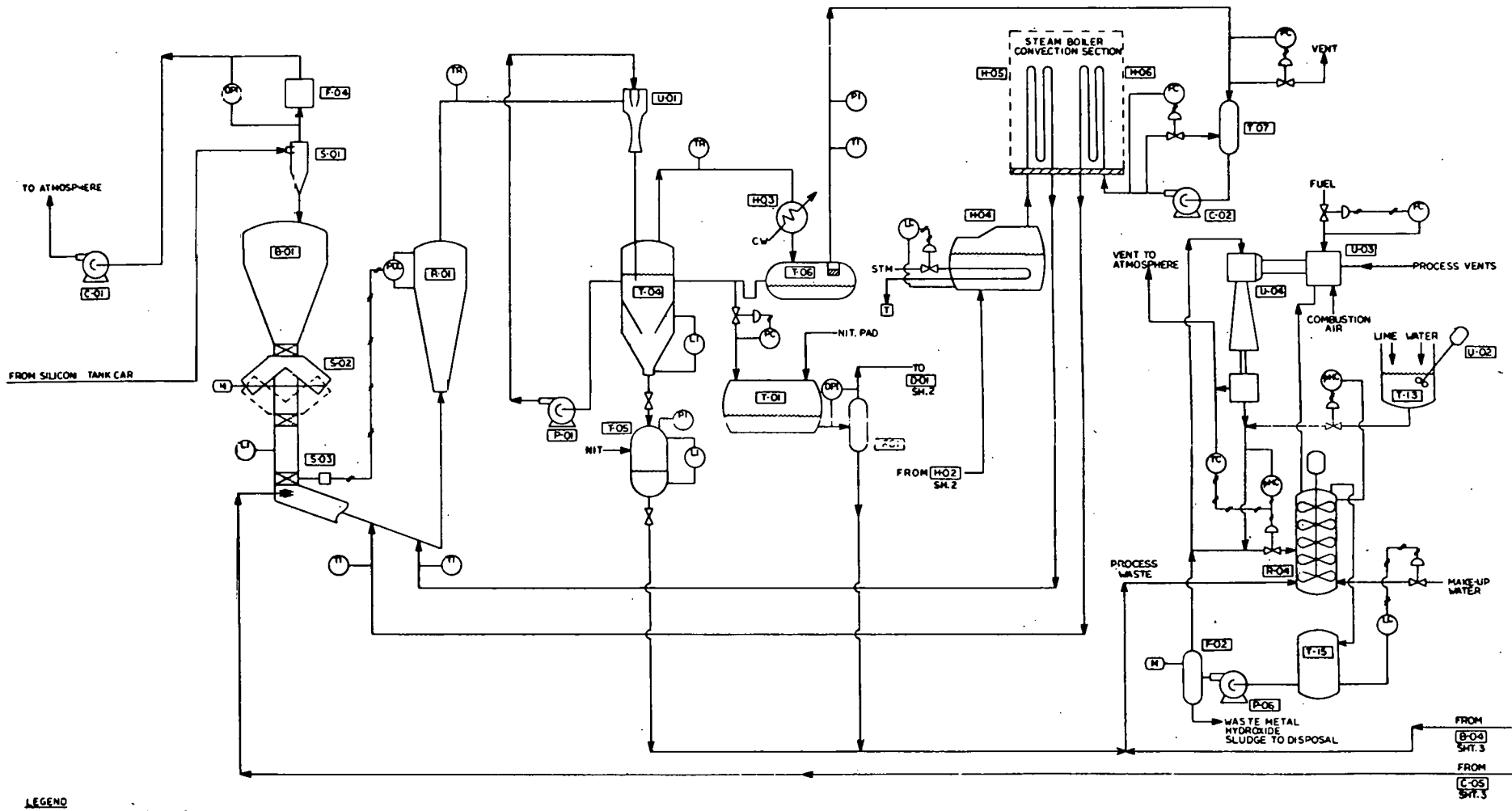


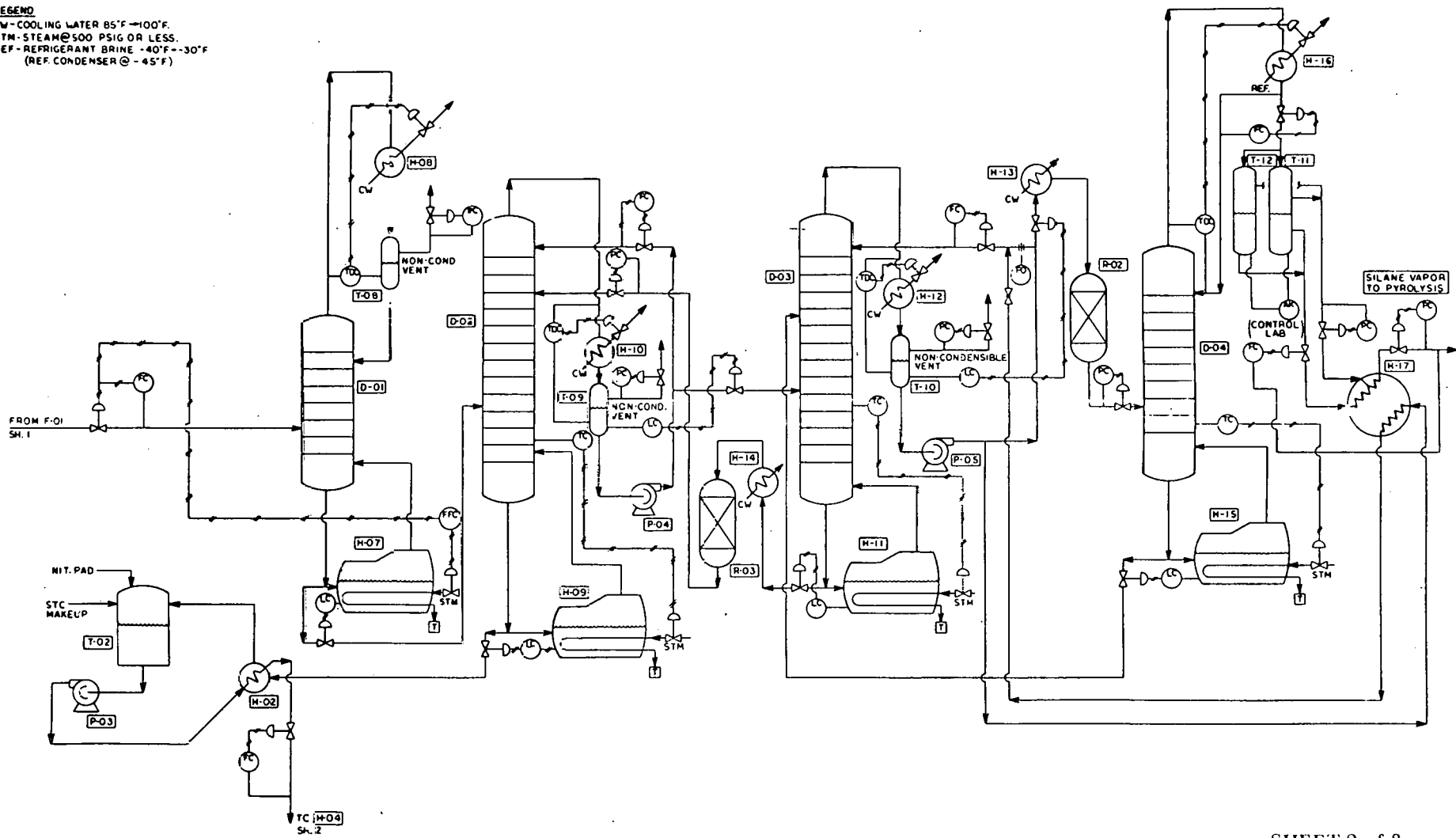
Figure 3.3

PRELIMINARY SGS PROCESS FLOW DIAGRAM FOR 1000 MT/YR PLANT HYDROGENATION/WASTE DISPOSAL

LEGEND
CW-COOLING WATER 65°F -105°F
STM-STEAM 500 PSIG OR LESS
REF-REFRIGERANT BRINE -40°F - -30°F
(REF. CONDENSER @ 45°F)

SHEET 1 of 3

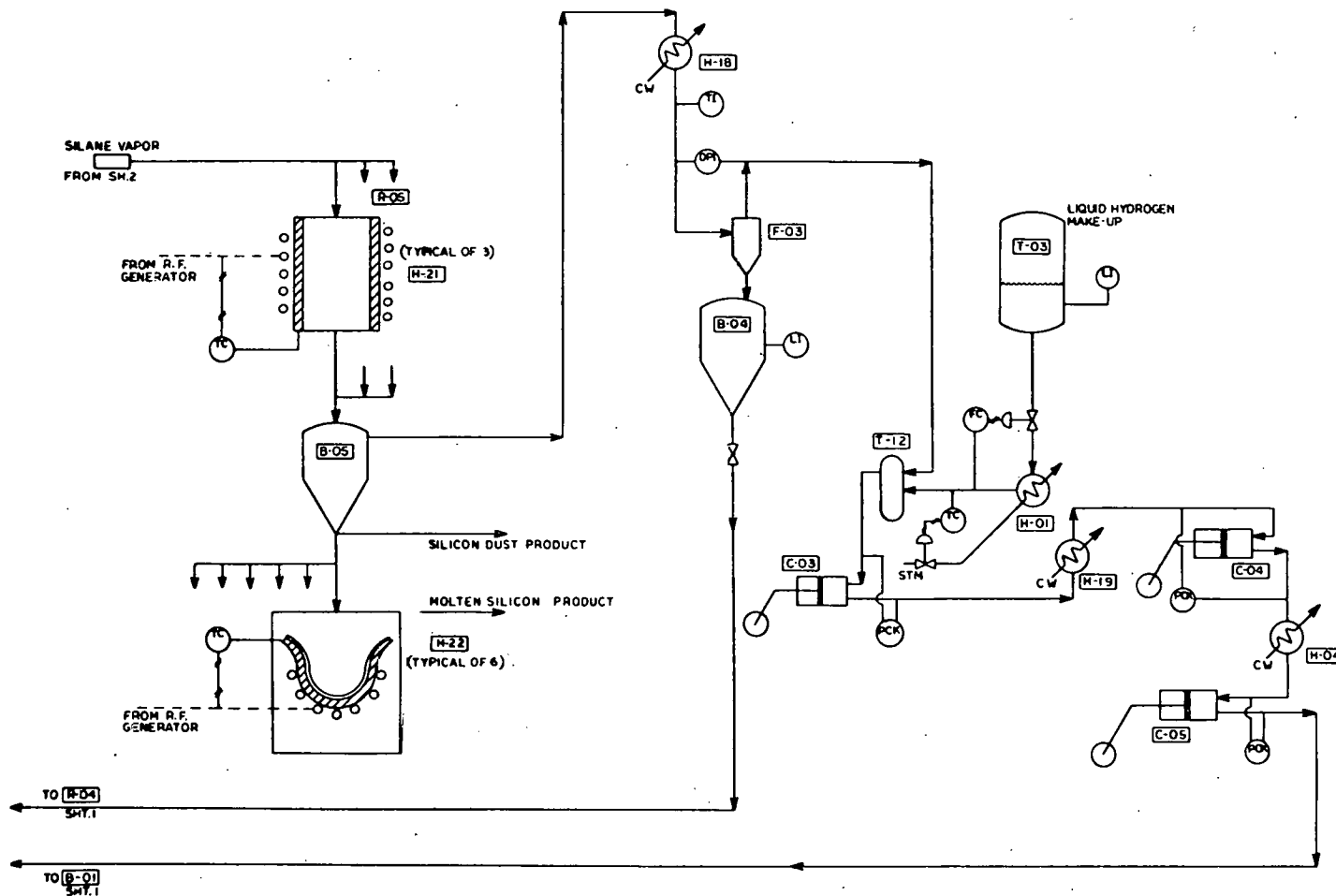
LEGEND
CW - COOLING WATER 85°F → 100°F.
STM - STEAM @ 500 PSIG OR LESS.
REF - REFRIGERANT BRINE -40°F → -30°F
(REF. CONDENSER @ -45°F)



SHEET 2 of 3

Figure 3.3 (Cont'd)

**PRELIMINARY SGS PROCESS FLOW DIAGRAM FOR 1000 MT/yr PLANT
DISTILLATION/REDISTRIBUTION**



LEGEND

CW-COOLING WATER 65°F -100°F

STM-STEAM @ 500 PSIG OR LESS

REF-REFRIGERANT BRINE -40°F--30°F
(REF. CONDENSER @ 45°F)

SHEET 3 of 3

Figure 3.3 (Cont'd)

PRELIMINARY SGS PROCESS FLOW DIAGRAM FOR 1000 MT/YR PLANT

PYROLYSIS/CONSOLIDATION

the Distillation Silane Process since one column and one reactor have been eliminated. Unlike the Adsorption Silane Process, this scheme does not require an activated carbon adsorption bed for final silane cleanup. This hybrid silane process scheme has been incorporated into the SGS (semiconductor-grade silane/silicon) Process. All future work will be based on this process scheme. A brief process description is presented below.

Starting with Sheet 1 of Figure 3.3, metallurgical-grade silicon is transported pneumatically from a tank car to a storage hopper (B-01) via a cyclone (S-01). It will be fed to a double-shell blender (S-02) and mixed with the hydrogenation copper catalyst. It is then fed through a lock hopper (S-03) batchwise to the hydrogenation reactor (R-01) at 500 psig. A mixture of silicon tetrachloride (STC) and hydrogen at 550°C is continuously fed to the reactor. The silicon is reacted to trichlorosilane (TCS) and the impurities to their respective chlorides. The hot effluent gases from the reactor are quenched to their dew point in a quench-contact ejector (U-01). The solids (insoluble metal chlorides) fall to the bottom of a settler (T-04) and are periodically withdrawn to a chemical treatment plant with lime (R-04).

The saturated vapors are then partially condensed to about 35°C and the condensate is collected in a storage tank (T-06 to T-01). Non-condensed vapors and hydrogen are heated (H-06) and recycled to the hydrogenation reactor (R-01). The crude TCS/STC condensate in the storage tank (T-01)

is fed to a stripping column (D-01 in Sheet 2) to remove the dissolved gases. The column bottoms are fed to a distillation column (D-02) operating at 55 psia.

The distillate is sent back to the STC make-up tank (T-02) and then is heated to 550°C before being recycled to the hydrogenation reactor. The TCS distillate containing some dichlorosilane (DCS) is fed to the next distillation column (D-03) where DCS and TCS are separated. The TCS bottoms are cooled and reacted in a catalytic reactor (R-03) at 85 psia to yield DCS and STC, which is sent back to the previous distillation column (D-02). The DCS distillate from the column (D-03) is cooled and reacted in the other catalytic reactor (R-02) at 550 psia to yield TCS and silane. This mixture is fed to a final distillation column (D-04) at 360 psia where the silane is separated from any chlorosilanes or other impurities. The TCS bottoms are returned to the previous column (D-03). The ultra-pure silane distillate product is stored in one of the two silane shift tanks (T-11, T-12).

The silane from the tank is vaporized (H-17) and fed to the pyrolysis reactor (R-05, Sheet 3) where it is decomposed to silicon powder and hydrogen. Hydrogen is separated in a silicon powder storage bin (B-05) and is sent back to the hydrogenation reactor after cleanup and pressurization. To make up for hydrogen losses, liquid hydrogen (T-03) is vaporized and compressed (C-03, C-04, C-05). To make up for chlorine losses, technical grade STC is periodically added to the STC

storage tank (T-02). The ultra-pure silicon powder is transported from the storage bin to the melter (H-22) where polycrystalline silicon product is produced.

The process for a 25 MT/yr experimental facility is almost identical to the 1000 MT/yr commercial process just described. Hydrogen, after pyrolysis, will not be recycled in a small experimental facility, however.

3.2.4b SCALE MODEL

A $\frac{1}{4}":1'$ scale model was constructed based on the plot shown in Figure 3.4. The scale model, shown in Figure 3.5 was quite useful in generating the plant cost and will be used extensively in future engineering work.

3.2.5 PRELIMINARY COSTS of 25, 50, 100 and 1000 MT/YR PLANTS

A detailed estimate was made by our Cost Engineering Department using the scale model of the commercial plant as the basis. The cost of a 1000 MT/yr plant is six million dollars. If we assume a 15-year plant life, 10-year sum-of-the-digit depreciation, 48% federal income tax, and 25% ROI after taxes, product selling price in 1975 dollars is \$6.45 per kg of molten silicon of 100 ohm-cm resistivity. This price is well below the 1986 cost goal of \$10/kg, in 1975 dollars, set by DOE/JPL.

Cost estimates were also performed for the 25, 50, and 100 MT/yr experimental facilities. The costs, scaled

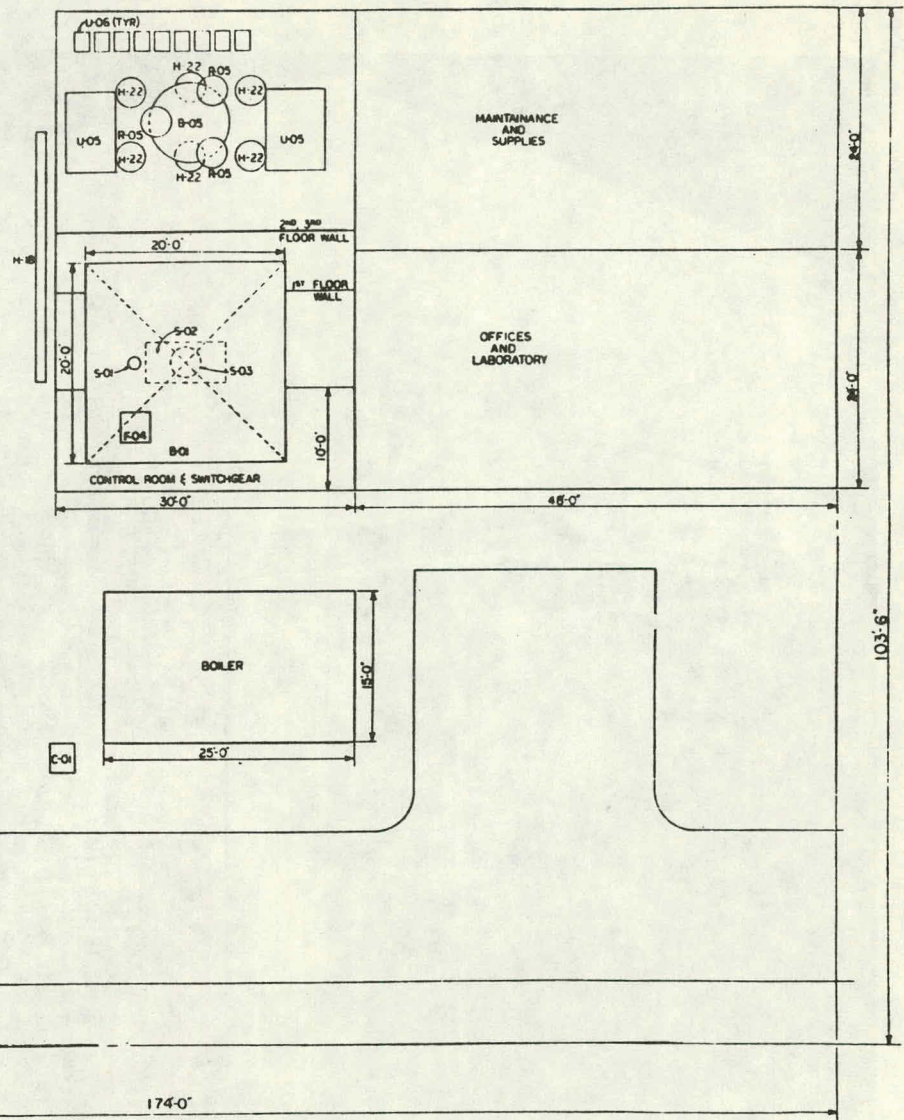
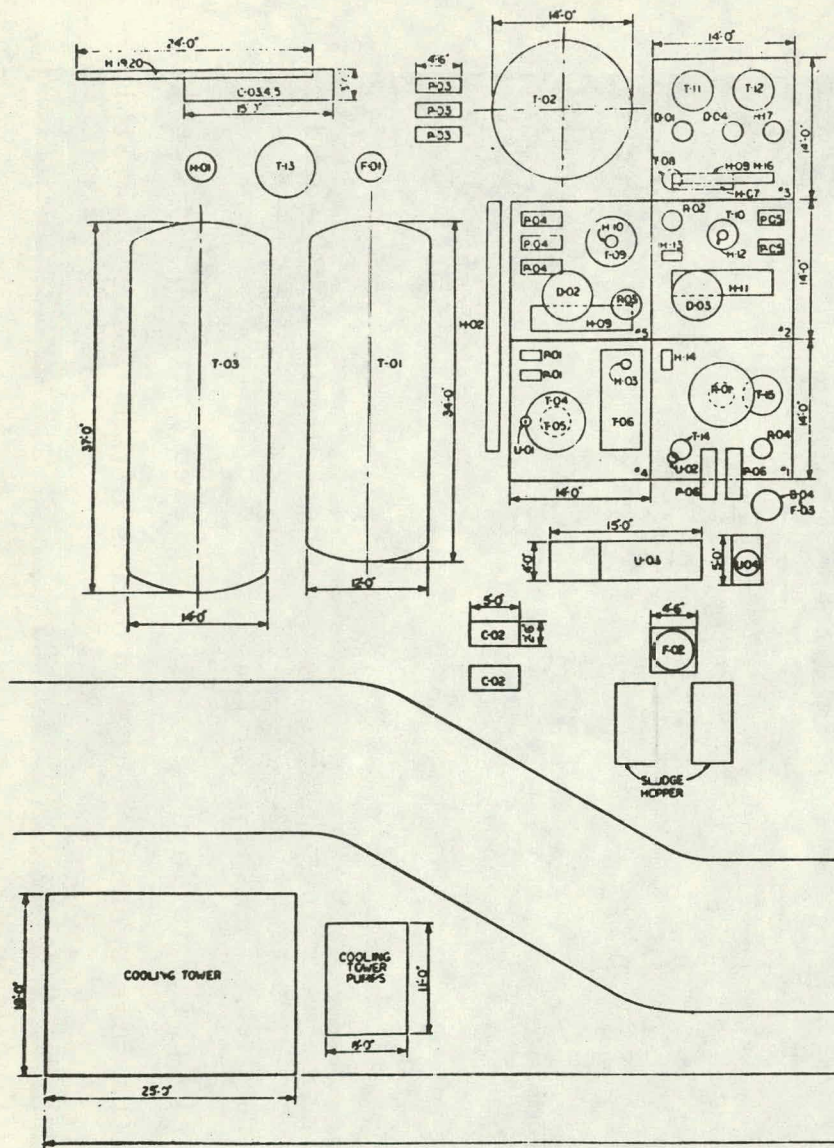


Figure 3.4 PLOT PLAN FOR THE 1000 MT/YR SGS PLANT

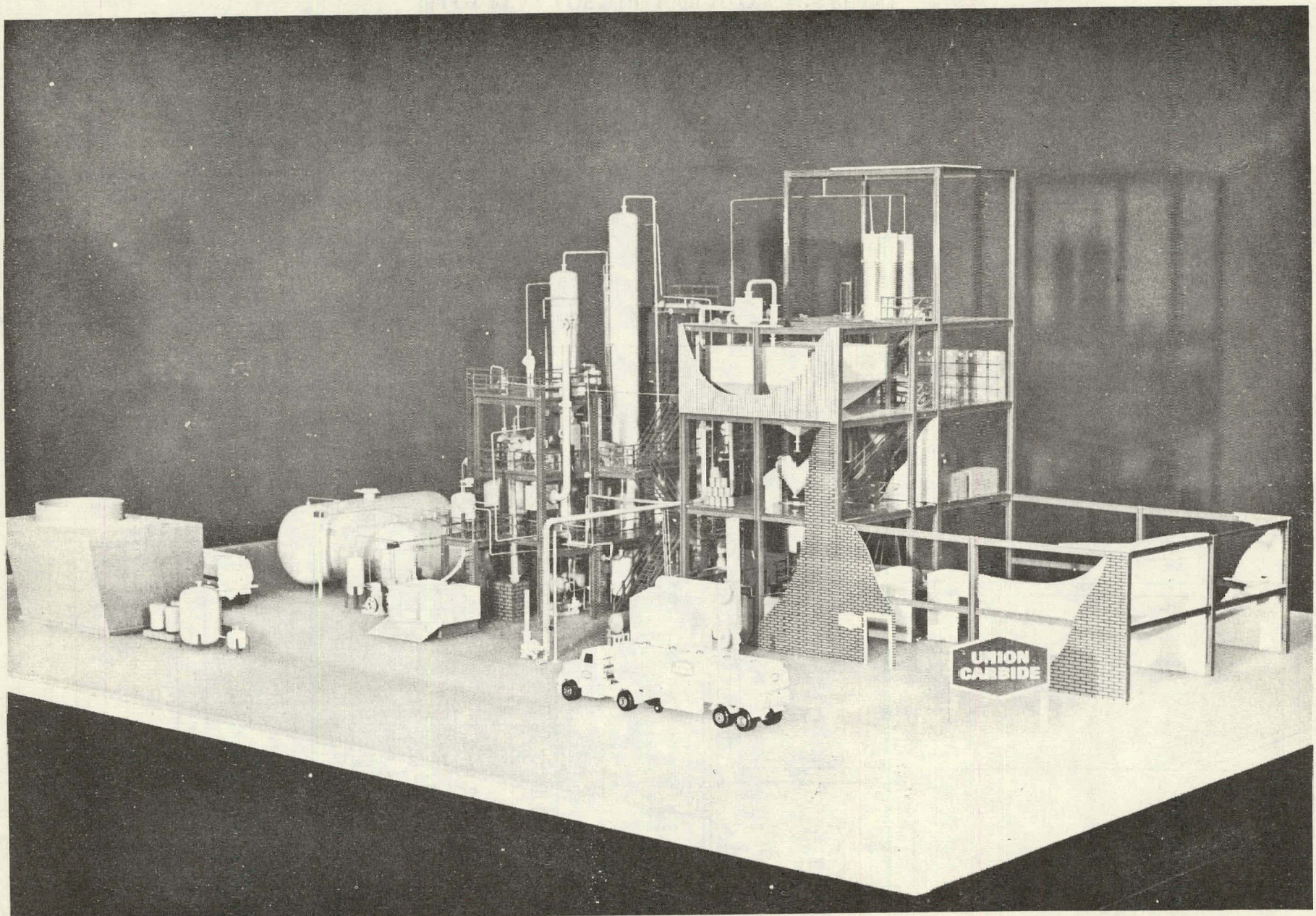


Figure 3.5
SCALE MODEL OF THE 1000 MT/YR PLANT

Table 3.2
PRODUCT PRICE FROM A 1000 MT/YR SGS COMMERCIAL PLANT

WORK PERFORMED UNDER JPL/DOE CONTRACT 954334

PLANT SIZE:	1000 METRIC TONS/YEAR	
ESTIMATED STREAM FACTOR:	85%	
PRODUCT QUALITY:	100 ohm-cm, AS MOLTEN SILICON	
PLANT AREA (AS SHOWN):	240' x 170' ~ 1 ACRE	
ESTIMATED PLANT COST (1978 DOLLARS):	\$6,000,000	
COSTS		\$/kg
RAW MATERIALS:	METALLURGICAL-GRADE SILICON HYDROGEN TECHNICAL-GRADE SILICON TETRACHLORIDE COPPER CEMENT CATALYST LIME	2.03
LABOR:	4 OPERATORS/SHIFT 1 LABORER/SHIFT 1 FORMAN/SHIFT 6 MAINTENANCE MEN/SHIFT	0.79
UTILITIES	20 MM Btu/hr COOLING WATER 15 MM Btu/hr STEAM 4 MM Btu/hr DIRECT HEAT 1310 KW ELECTRICITY	0.75
MAINTENANCE:	ESTIMATED @ 7% PLANT COST	0.42
PROPERTY TAXES:	ESTIMATED @ 0.5% PLANT COST	0.03
INSURANCE:	ESTIMATED @ 1.0% PLANT COST	0.06
OPERATING COST, EXCLUDING DEPRECIATION		<u>\$4.08</u>
CAPITAL CHARGES*		<u>3.72</u>
PRODUCT PRICE - 1978 DOLLARS		\$7.80
- 1975 DOLLARS		\$6.45

* (15 YEAR PROJECT LIFE, 10 YEAR SYD DEPRECIATION, 48% FEDERAL INCOME TAX,
100% EQUITY FINANCING, 2 YEARS CONSTRUCTION TIME, 25% DCF RATE).

from the 1000 MT/yr plant, are \$4.0, \$4.2, and \$4.5MM for the 25, 50, and 100 MT/yr plants, respectively. Table 3.3 shows the product prices for various size plants based on various financing methods. Product price ranges a great deal depending on the financing method. For example, product price from a 1000 MT/yr plant in 1978 dollars ranges from \$7.80/kg (100% equity financing, 25% ROI) to \$4.96/kg (100% public financing, 9% interest on debt). The table also shows that 50/50 equity/public financing with 25% ROI on equity gives a product cost from a 100 MT/yr plant of \$30.26/kg in 1978 dollars or \$25.01 per kg in 1975 dollars. This product cost will meet the DOE/JPL interim cost goal of \$25/kg by 1982. If 100% public financing with 9% interest on debt is used, the product cost from a 100 MT/yr plant is even lower, \$22.48/kg in 1978 dollars or \$18.58/kg in 1975 dollars.

A sensitivity analysis of the plant cost on the product cost was also made. If we use equity financing with 25% ROI, the product cost increment is \$0.50/kg per each million-dollar increase in plant cost. It is clear that the plant cost can go up substantially and still meet the 1986 cost goal.

3.2.6 PROCESS DESIGN DATA

3.2.6a PHYSICAL and CRITICAL PROPERTIES of SILANE and CHLOROSILANES

A literature search was conducted for thermodynamic and physical properties of silane and the

Table 3.3
PRODUCT PRICES FOR VARIOUS PLANT SIZES, FINANCES
IN 1978 DOLLARS

BASIS:

25, 50, 100 MT/Y PILOT PLANT
 1000 MT/Y COMMERCIAL PLANT
 START-UP @ 10% CAPITAL INVESTMENT
 WORKING CAPITAL @ 30% ANNUAL OPERATING COST
 15 YEAR PROJECT LIFE
 48% FEDERAL INCOME TAX RATE
 2 YEARS CONSTRUCTION TIME
 9% INTEREST ON DEBT
 ANNUAL MAINTENANCE @ 7% OF CAPITAL INVESTMENT
 ANNUAL TAXES AND INSURANCE @ 1.5% OF CAPITAL INVESTMENT

<u>PLANT SIZE</u>	<u>25</u>	<u>50</u>	<u>100</u>	<u>1000</u>
<u>10 YEARS SYD DEPRECIATION, 100% EQUITY FINANCING</u>				
PRICE, \$/Kg @ 15% DCF	100.60	54.59	30.85	6.18
@ 25% DCF	140.38	75.78	42.17	7.80
<u>15 YEARS STRAIGHT-LINE DEPRECIATION, 100% EQUITY FINANCING</u>				
PRICE, \$/Kg @ 15% DCF	106.11	57.51	32.40	6.39
@ 25% DCF	147.72	79.68	44.24	8.08
<u>15 YEARS STRAIGHT-LINE DEPRECIATION, 75% EQUITY FINANCING</u>				
PRICE, \$/Kg @ 15% DCF	91.14	49.54	28.15	5.80
@ 25% DCF	113.68	61.57	34.59	6.74
<u>15 YEARS STRAIGHT-LINE DEPRECIATION, 50% EQUITY FINANCING</u>				
PRICE, \$/Kg @ 15% DCF	84.34	45.91	26.20	5.51
@ 25% DCF	98.51	53.47	30.26	6.10
<u>15 YEARS STRAIGHT-LINE DEPRECIATION, 25% EQUITY FINANCING</u>				
PRICE, \$/Kg @ 15% DCF	77.74	42.39	24.31	5.23
@ 25% DCF	84.40	45.95	26.22	5.51
<u>15 YEARS STRAIGHT-LINE DEPRECIATION, 100% PUBLIC FINANCING</u>				
PRICE, \$/Kg	71.35	38.98	22.48	4.96

chlorosilanes. The data found was correlated and reduced to a uniform set of physical properties which is intended to serve as the data base for the process design of the Low Cost Solar Array (LSA) Project silicon/silane plant. The constants necessary to utilize the in-house process computer system PROBE for physical property calculations were also derived from the correlations. This work was documented in a departmental engineering memorandum. (3.7)

3.2.6b PROCESS DESIGN DATA ACQUISITION

The process design data needs were identified and documented in December 1977. (3.2, 3.9) Since then, a comprehensive literature survey (both in-house and open sources) was conducted. The study was reviewed with the objective of limiting experimental work as much as possible while still maintaining our ability to design the plant accurately.

This work resulted in a revised document (3.9) on the process design data needs. Data needs include chlorosilanes heats of formation, equilibrium and kinetic performance of the hydrogenation reactor, chlorosilane catalytic redistribution equilibrium and kinetics, chlorosilanes binary VLE, and chlorosilanes/impurities VLE. The Union Carbide Chemicals and Plastics South Charleston thermodynamic laboratory and the C and P Sistersville Silicones Plant have been identified in combination as appropriate locations for obtaining all of the needed data.

Arrangements necessary for starting the experimental work were completed. It is anticipated that all results should be available by September 1978. Preparations are being made to incorporate new data into the process design computer systems (PROBE and MDCC) as quickly as they become available.

3.3 CONCLUSIONS

A critical review of the two candidate silane process schemes resulted in yet another hybrid process scheme, which requires fewer pieces of equipment than either of the earlier schemes. It has an excellent silane separation system and does not require an adsorption bed for final silane cleanup. This process scheme was selected and was incorporated into the Union Carbide SGS (Semiconductor-grade Silane/Silicon) process design.

A SGS process design package for the 25 MT/yr plant was completed and is in final review. The package contains the Detailed Process Description, Equipment Data Sheets, Heat and Mass Balance, Process Flow Diagram, Plant Layout Drawing, Electrical One-Line Drawing, and the Pyrolysis Unit Drawing.

Preliminary costs of the 25, 50, 100, and 1000 MT/yr plants were generated. The costs, scaled from the 1000 MT/yr plant estimate of \$6.0 million, are \$4.0, \$4.2, and \$5.0 million for the 25, 50, and 100 MT/yr plants, respectively. The product

selling price from a 1000 MT/yr plant is \$6.45/kg of semiconductor-grade silicon on \$6.0 million investment (DCF, 25% ROI). This price is well below the JPL/DOE 1986 cost goal of \$10/kg. There is a good chance that the product selling price from the 100 MT/yr plant will meet the interim cost goal of \$25/kg.

3.4 PROJECTED QUARTERLY ACTIVITIES

3.4.1 PRELIMINARY PROCESS DESIGN of 25 MT/YR EXPERIMENTAL FACILITY

We will complete inspection of the process design package and transmit it to JPL. The stream catalog and the complete heat and mass balance will be made. A tabular trace component system summary will be prepared for all major streams and calculational procedures will be established.

3.4.2 FINAL PROCESS DESIGN of EXPERIMENTAL FACILITY

The second and final pass of the SGS process design will be initiated. The process design will incorporate all new design data as they become available.

3.4.3 RESEARCH and DEVELOPMENT PROGRAM PLAN

We believe that the present pyrolysis/melting scheme will be acceptable in the experimental facility. However, it appears unsuited for a commercial plant application. We will assemble an R & D program which we plan to initiate as quickly as possible.

3.5 REFERENCES

- 3.1 H. Morihara, S. K. Iya, and E. J. McHale, "Process Design for the 25 MT/Yr Experimental Facility and Economic Analysis. High Frequency Capacitive Heating of Silicon Particles", Monthly Progress Report, JPL Contract 954334, Linde Division, Union Carbide Corporation, Tonawanda, New York, November, 1977.
- 3.2 W. C. Breneman, E. G. Farrier and H. Morihara, "Feasibility of a Process for Low-Cost, High-Volume Production of Silane to Semiconductor-Grade Silicon", Quarterly Progress Report, JPL Contract 954334, Union Carbide Corporation, October-December, 1977.
- 3.3 S. K. Iya, "Conceptual Design of Hydrogenation Reactor for 25 MT/Yr and 1000 MT/Yr Silicon Plant", Engineering Memorandum No. 6203 (SGS-8), Linde Division, Union Carbide Corporation, Tonawanda, New York, February 24, 1978.
- 3.4 R. A. Beddome, "Redistribution of Trichlorosilane Kinetic Performance of Rohm & Haas A-21 Amine Catalyst", Engineering Memorandum No. 6182 (SGS-6), Linde Division, Union Carbide Corporation, Tonawanda, New York, January 19, 1978.
- 3.5 F. S. DiPaolo, "Design of Activated Carbon Trap for Purification of Silane in 25 MT/Yr High Purity Silicon Metal Plant", Engineering Memorandum No. 6215 (SGS-10), Linde Division, Union Carbide Corporation, Tonawanda, New York, March 16, 1978.
- 3.6 R. A. Beddome, "25 MT/Yr Solar Cell Silicon Plant Process Description", Engineering Memorandum No. 6230 (SGS-12), Linde Division, Union Carbide Corporation, Tonawanda, New York, March 30, 1978.
- 3.7 T. E. Diegelman, "Physical and Critical Properties of Silane and the Chlorosilanes", Engineering Memorandum No. 6206 (SGS-9), Linde Division, Union Carbide Corporation, Tonawanda, New York, March 10, 1978.
- 3.8 R. A. Beddome, "Process Design Data Needs for High Purity Silane Production", Engineering Memorandum No. 6159 (SGS-5), Linde Division, Union Carbide Corporation, Tonawanda, New York, December 14, 1977.
- 3.9 R. A. Beddome, "Process Design Data Needs for High Purity Silane Production", Engineering Memorandum No. 6159A (SGS-5A), Linde Division, Union Carbide Corporation, Tonawanda, New York, February 22, 1978.

4.0 CAPACITIVE FLUID-BED HEATING

4.1 INTRODUCTION

This program is exploring the feasibility of utilizing electrical capacitive heating to control the fluidized silicon bed temperature during the heterogeneous decomposition of silane. In addition, a theoretical fluid-bed silicon deposition model is being developed to be used in a design of a fluid-bed pyrolysis process scheme.

In this reporting period, fluidization regimes of various particle-size ranges were observed experimentally with nitrogen, argon, and helium used as fluidization gases. The bed was heated capacitively and the temperature variations within the bed were measured.

The theoretical modelling work is nearing completion. An additional feature was added to the model and the analysis now includes the capability for handling cascading multiple beds. When the temperatures of the beds are increased from one bed to the next bed, a silane feed to the first bed may be essentially pure. This arrangement, if workable, may eliminate the hydrogen recycle. Based on this analytical model, a promising fluid-bed pyrolysis scheme was selected for a functional process design and an economic analysis.

4.2 DISCUSSION

4.2.1 ANALYTICAL MODEL

The purpose of the analytical study is to model heat and mass transfer in the fluid-bed pyrolysis reactor. The analysis consists of two parts. The first part is to find the heat and mass transfer across a thin stagnant boundary layer. This quasi one-dimensional model is then applied to the individual particles in the fluid-bed in the second part to determine the bed performance based on epitaxial silicon deposition data (very dilute silane).

The analysis yields the following information. It is known that at any given temperature there is a critical concentration of silane above which free-space decomposition occurs. The critical concentration is plotted against the bed temperature. As shown in Figure 4.1, the critical silane concentration is independent of heating methods up to 1100°K . Above that temperature particle heating allows a higher silane concentration. The condition exists under which the concentration of silane in the stagnant layer around the bed particle is always under the critical concentration. The maximum concentration is plotted against the distance from the particle surface. The critical concentration is superimposed on the plot to show that the maximum concentration line is tangent to the critical concentration at some distance from the surface. The analysis also yields the maximum throughput as functions of particle temperatures and boundary-layer thickness. As the layer thickness increases, there is a transition from the reaction-limited to diffusion-limited deposition.

Figure 4.2 gives the power input to the fluid-bed as a function of the particle temperature. It teaches us that the bed temperature must be low (say 950°K) for a low energy operation. At this low temperature, the analysis shows that the bed height can be quite reasonable (Figure 4.3) and that the bed diameter is small (Figure 4.4). However, the deposited surface would be porous. Whether porous particles can be accepted as the final product and whether they can promote self-seeding must be determined.

The possibility of cascading multiple beds was added to the model. This was done by constraining each bed to convert enough silane to feed the next bed with a mixture lean enough that homogeneous decomposition does not occur. The overall reactor constraints are total conversion efficiency and inlet concentration. The program results are the dimensions of each bed and the power and heat recovery requirements generated in each bed.

A primary motivation for investigating cascading beds was the possibility of feeding the reactor with essentially pure silane and thus avoid having to recycle hydrogen around the fluid-bed. In a single isothermal bed, this would lead to a prohibitively long reactor for reasonable size particles.

The distribution of temperatures in each bed is optimized by a simple parabola-fitting minimization program. This

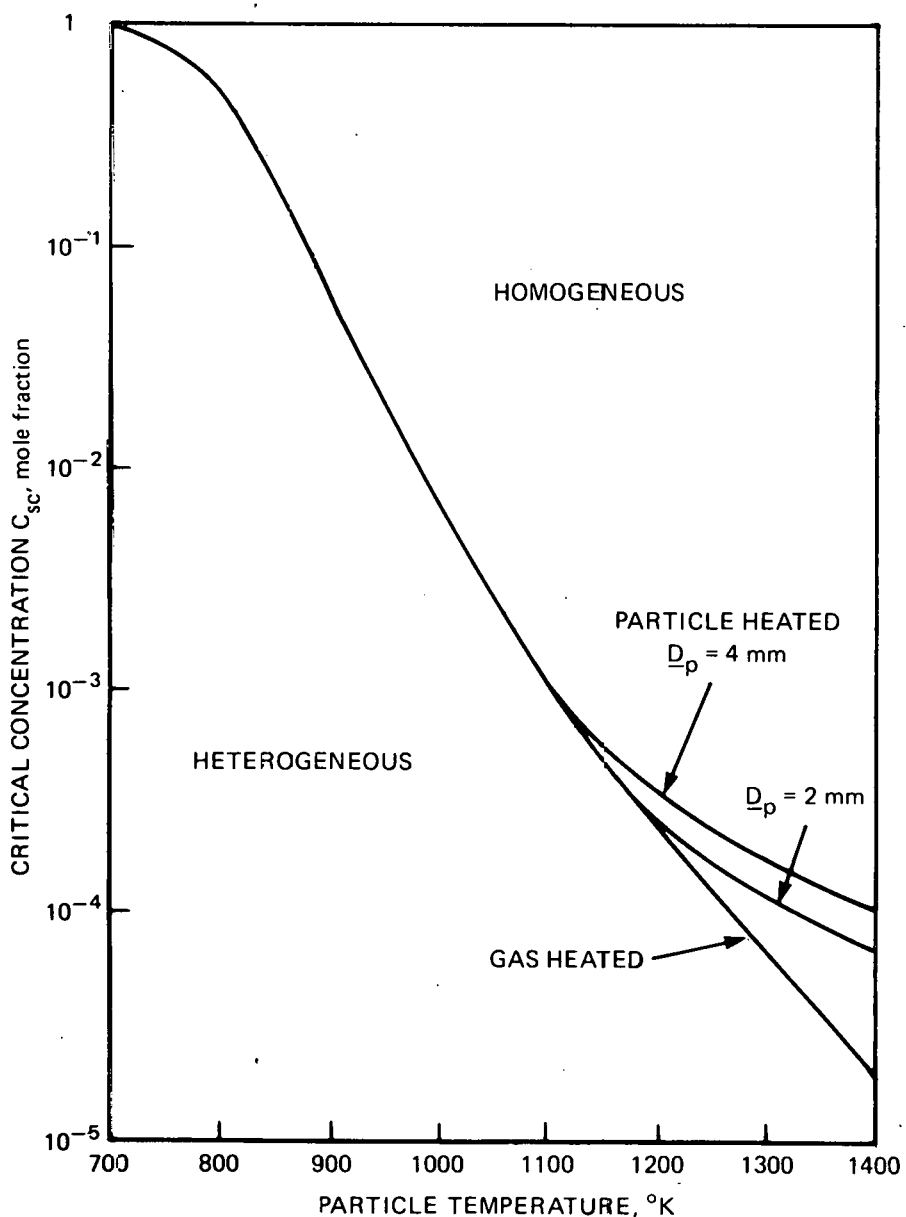


Figure 4.1
CRITICAL SILANE CONCENTRATION vs TEMPERATURE

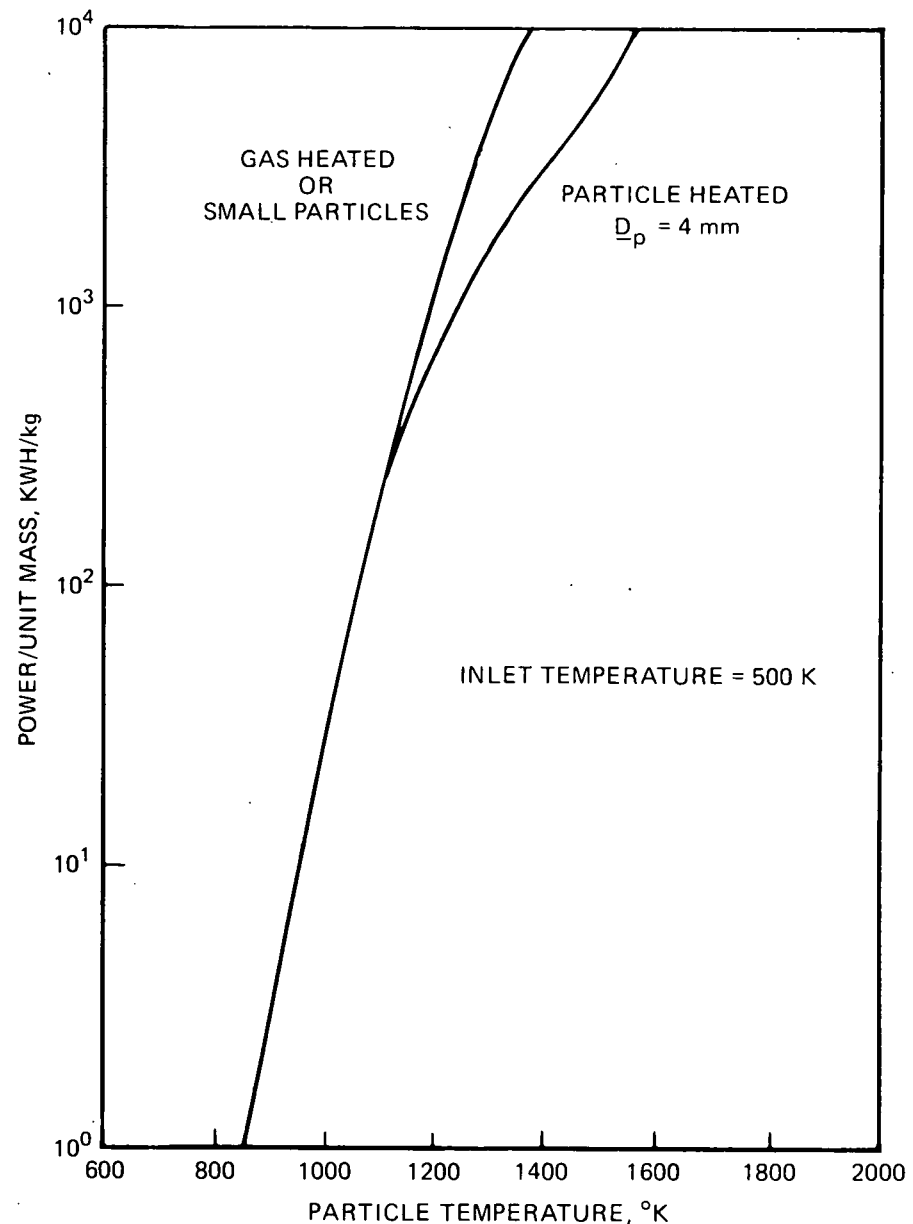


Figure 4.2
POWER REQUIREMENT PER KILOGRAM PRODUCT
vs TEMPERATURE OF PARTICLE

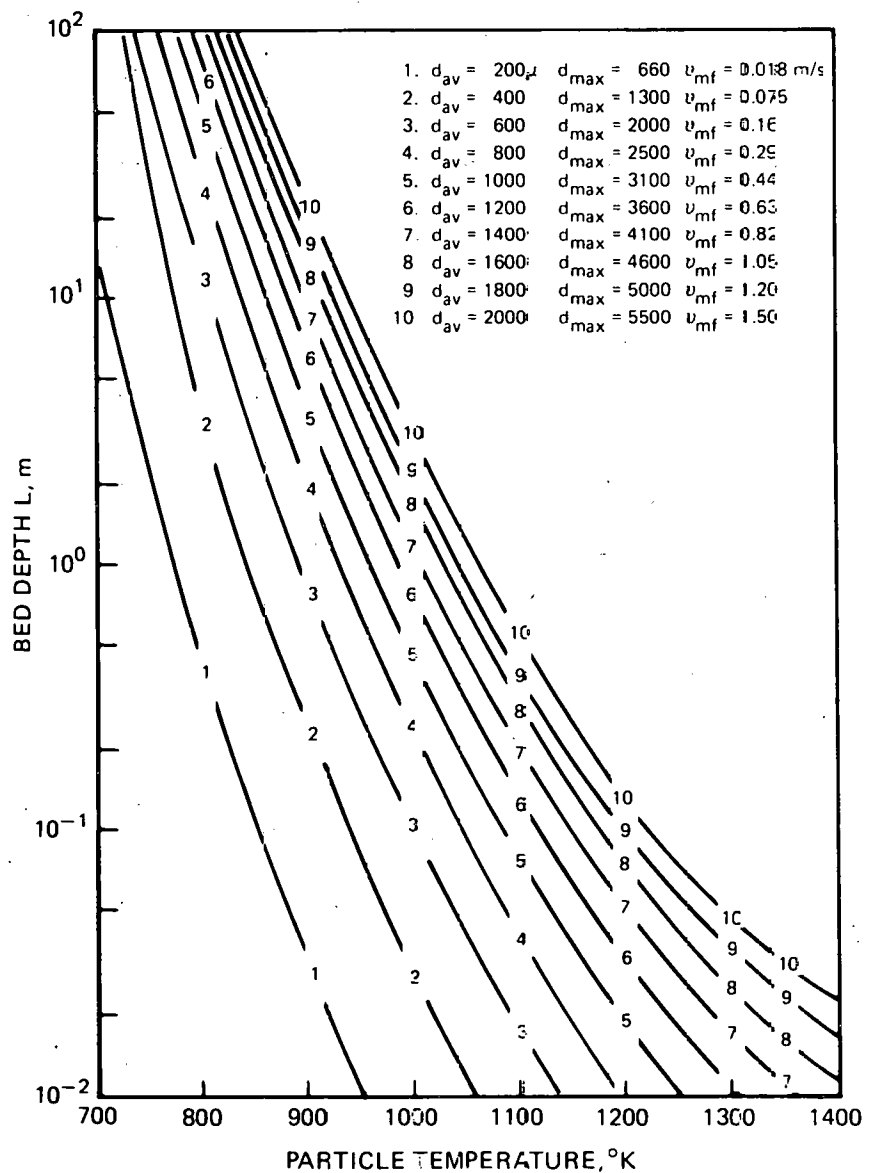


Figure 4.3
BED DEPTH vs TEMPERATURE
FOR 99% CONVERSION OF SILANE TO SILICON

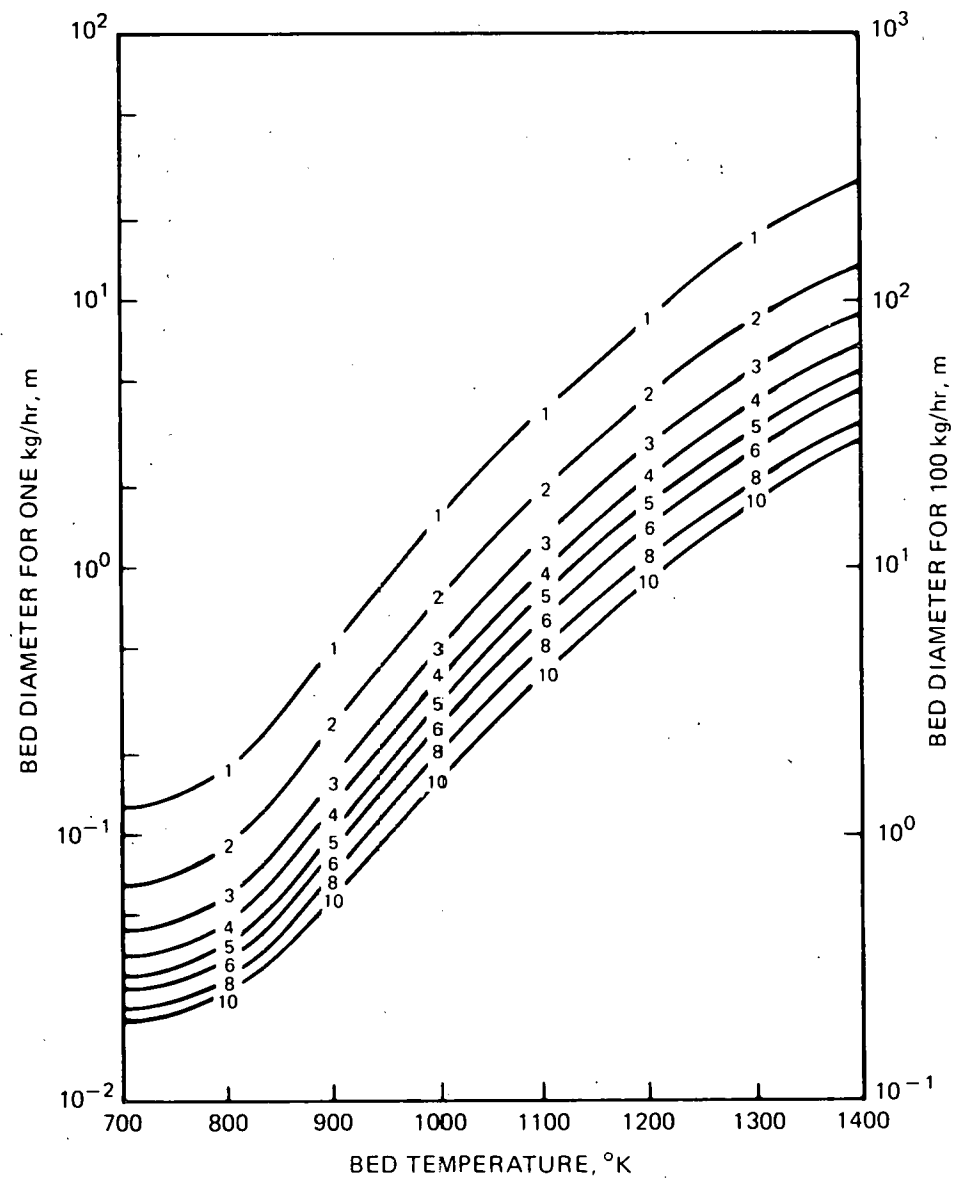


Figure 4.4
REACTOR DIAMETER vs BED TEMPERATURE

results in a reactor with the minimum possible overall length for a given inlet silane concentration. The results so far are encouraging.

The analytical model yielded several promising process schemes, one of which was selected as a base case. A functional design of the base case and the economic analysis will be initiated shortly.

4.2.2 EXPERIMENTAL STUDY

4.2.2a FLUIDIZATION CHARACTERISTICS

The observed fluidization characteristics of a bed of 500 to 1000 μm particles are shown in Table 4.1. The minimum fluidization velocity (V_{mf}) computed from the Ergun equation is 0.375 m/s. The voidage of the bed at the minimum fluidization velocity was found to be 0.6. These tests were repeated with the particle-size range, bed depth, and type of gas as variables. The test results are presented in Table 4.2. The predicted values of V_{mf} for silicon particles in nitrogen, argon, helium, and hydrogen at 25°C and 700°C are shown in Figure 4.5. The observed values, for the most part, match with the predicted ones quite well.

4.2.2b ELECTRICAL PHENOMENA

The electrical behavior of the silicon bed is classified into two states. In the first state, the current conducted by the bed at a fixed voltage is substantially independent of frequency in the range examined. The impedance of the bed is about 10 ohms. This state is called the L-state (low resistance).

Table 4.1
OBSERVED FLUIDIZATION CHARACTERISTICS OF A BED

500-1000 μm MESH PARTICLE
 ROOM-TEMPERATURE NITROGEN
 MINIMUM FLUIDIZATION VELOCITY = 0.375 m/s

NITROGEN VELOCITY (m/s)	DESCRIPTION OF BED	BED HEIGHT (mm)
0	NO MOVEMENT	143
0.195	NO MOVEMENT	143
0.293	SLIGHT MOVEMENT AT BED TOP	149
0.342	UPPER 25mm OF BED MOVING; MIDDLE AND BOTTOM INACTIVE	154
0.391	BUBBLING BED; GRAINS MOVING RAPIDLY EXCEPT FOR LOWER 35mm WHERE PARTICLES ARE HARDLY MOVING	167
0.440	BED VERY ACTIVE, SAVE LOWER 32mm WHERE MOVEMENT IS RELATIVELY SLOW	179-186
0.489	LARGER BUBBLES; GROSS OSCILLATIONS IN FLOW METER; ALMOST ALL BED VERY ACTIVE	198-211
0.587	VERY ACTIVE	214-251
0.685	VERY ACTIVE	222-294

Table 4.2
OBSERVED AND PREDICTED MINIMUM FLUIDIZATION VELOCITIES

PARTICLE SIZE (μm)	BED DEPTH (mm)	GAS	V _{mf} OBSERVED (m/s)	V _{mf} CALCULATED (m/s)
600 - 1200	107	N ₂	0.62	0.19 - 0.92
	107	A	0.44	0.16 - 0.80
	107	He	0.49	0.17 - 0.83
	170	N ₂	0.54	0.19 - 0.92
	170	A	0.43	0.16 - 0.80
	170	He	0.67	0.17 - 0.83
	240	N ₂	0.40	0.16 - 0.80
	240	A	0.36	0.17 - 0.83
	240	He	0.56	0.19 - 0.92
	360	N ₂	0.38	0.16 - 0.80
250 - 600	360	A	0.36	0.17 - 0.83
	360	He	0.56	0.19 - 0.92
	114	N ₂	0.13	0.045 - 0.16
	114	A	0.16	0.036 - 0.17
	114	He	--	0.041 - 0.19
	177	N ₂	0.19	0.045 - 0.16
	177	A	0.13	0.036 - 0.17
	177	He	0.35	0.041 - 0.19
	244	N ₂	0.16	0.045 - 0.16
	244	A	0.16	0.036 - 0.17
	244	He	0.38	0.041 - 0.19

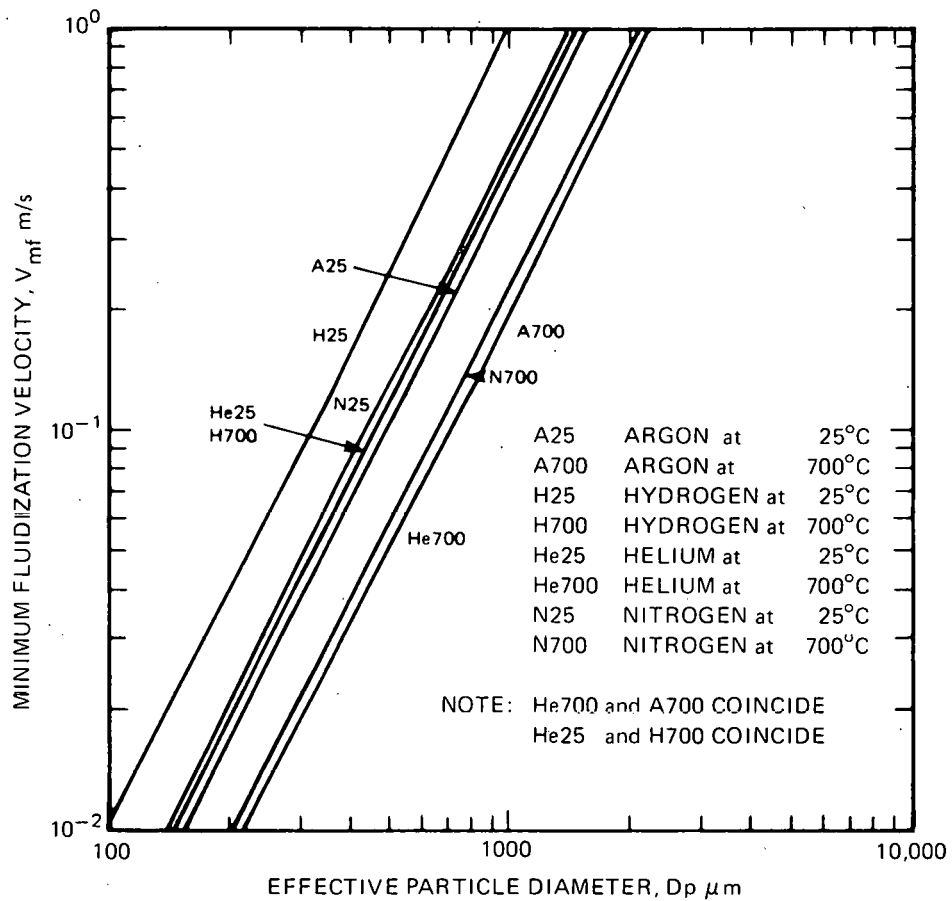


Figure 4.5
MINIMUM FLUIDIZATION VELOCITY vs EFFECTIVE
PARTICLE DIAMETER FOR SILICON PARTICLES

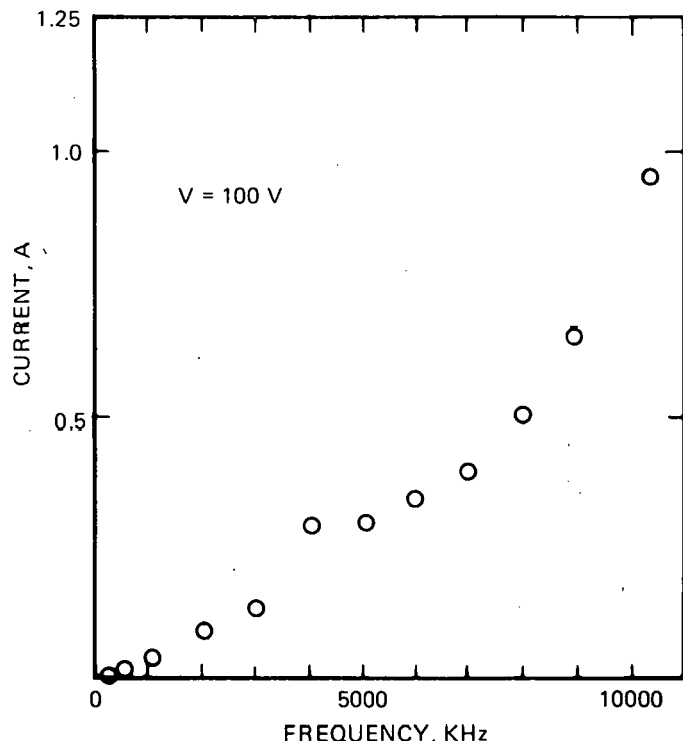


Figure 4.6
CURRENT vs FREQUENCY OF BED IN STATE H

In the second state (the H-state), the current increases with frequency. At 2.5 MHz, the impedance is about 200 ohms. Figures 4.6 and 4.7 give the experimental data relating the current vs frequency of the bed in State H and State L, respectively.

We have been unable to postulate any mechanism that accounts for these two states. There appears to be no correlation with temperature, bed depth, flow rate, or reactor type. Earlier tests seemed to indicate a particular temperature of transition at about 35°C. Subsequent tests at more widely varying conditions failed to substantiate this. A possibly important variable which has not been tried is changing the silicon purity and the method of particle preparation. It has been assumed that the normal state of the silicon bed is the L-state.

4.2.2c TEMPERATURE MEASUREMENT

The thermocouples used in a bed have metal sheathes which are coated with ceramic cement (Figure 4.8). This has been found to eliminate RF noise and prevent the sheath from shorting out the portion of the bed nearby.

The first series of tests was conducted to see if the power input matches the power output. As shown in Figure 4.9, when allowance was made for phase difference between voltage and current, it was possible to balance the thermal power ($\dot{m} C_p \Delta T$) and the electrical power.

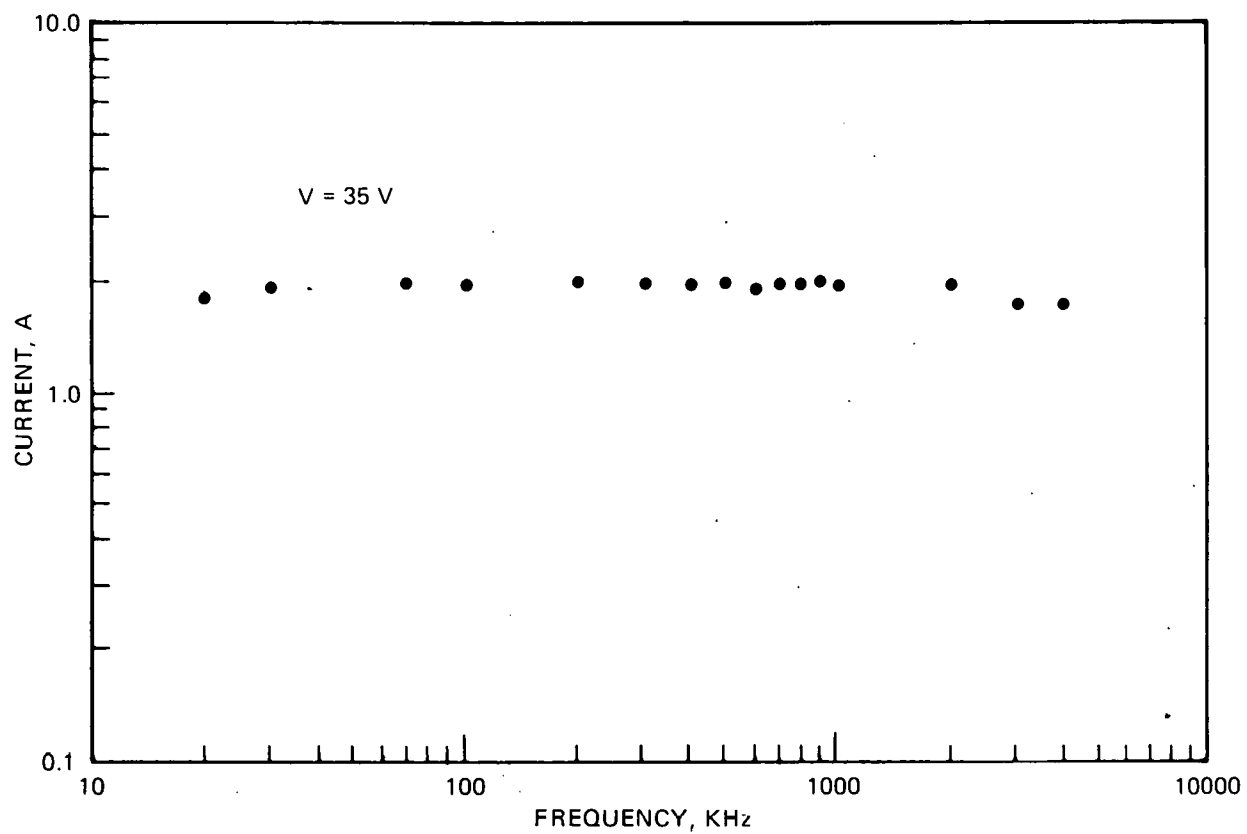


Figure 4.7
CURRENT vs FREQUENCY OF BED IN STATE L

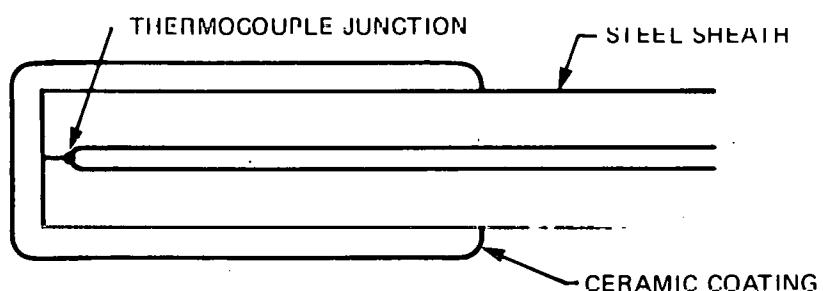


Figure 4.8
SKETCH OF COATED ELECTRODE

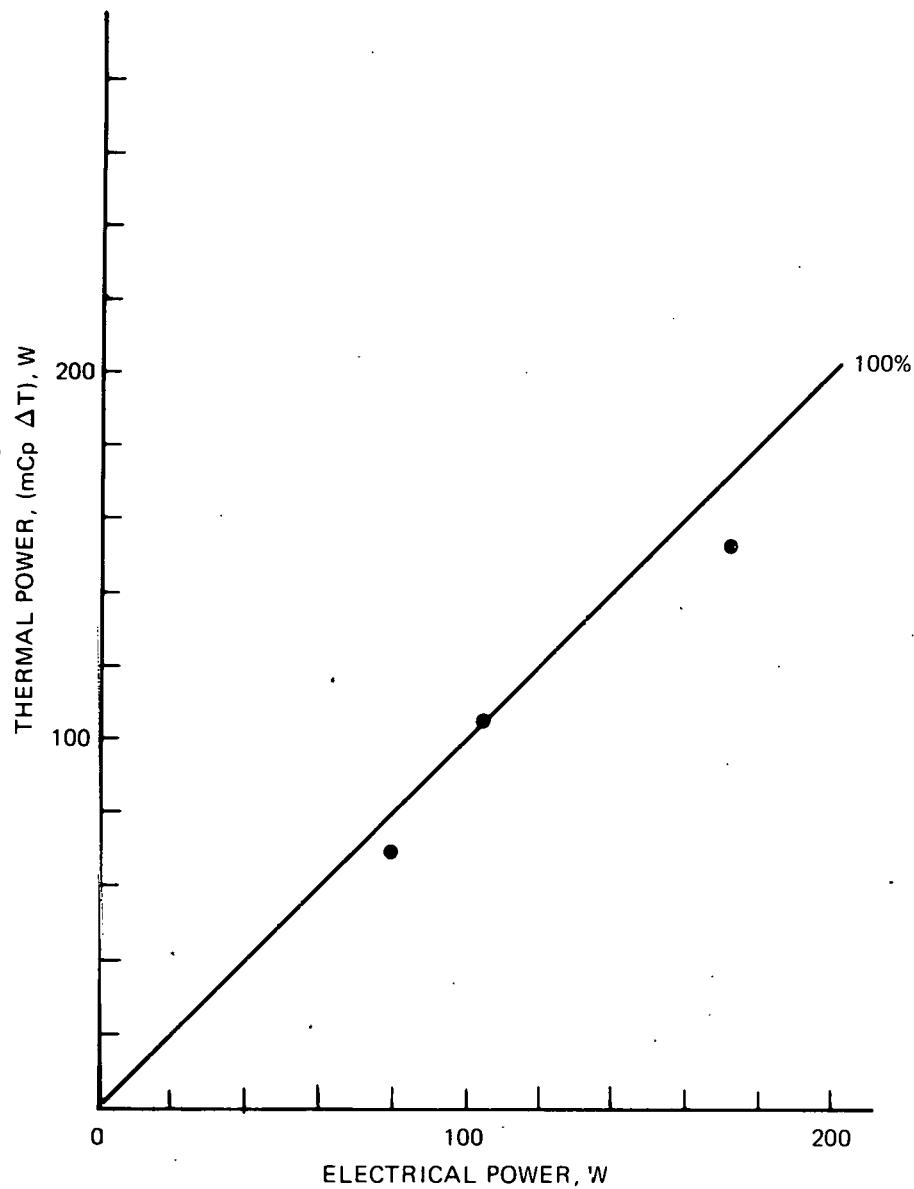


Figure 4.9
THERMAL vs ELECTRICAL POWER

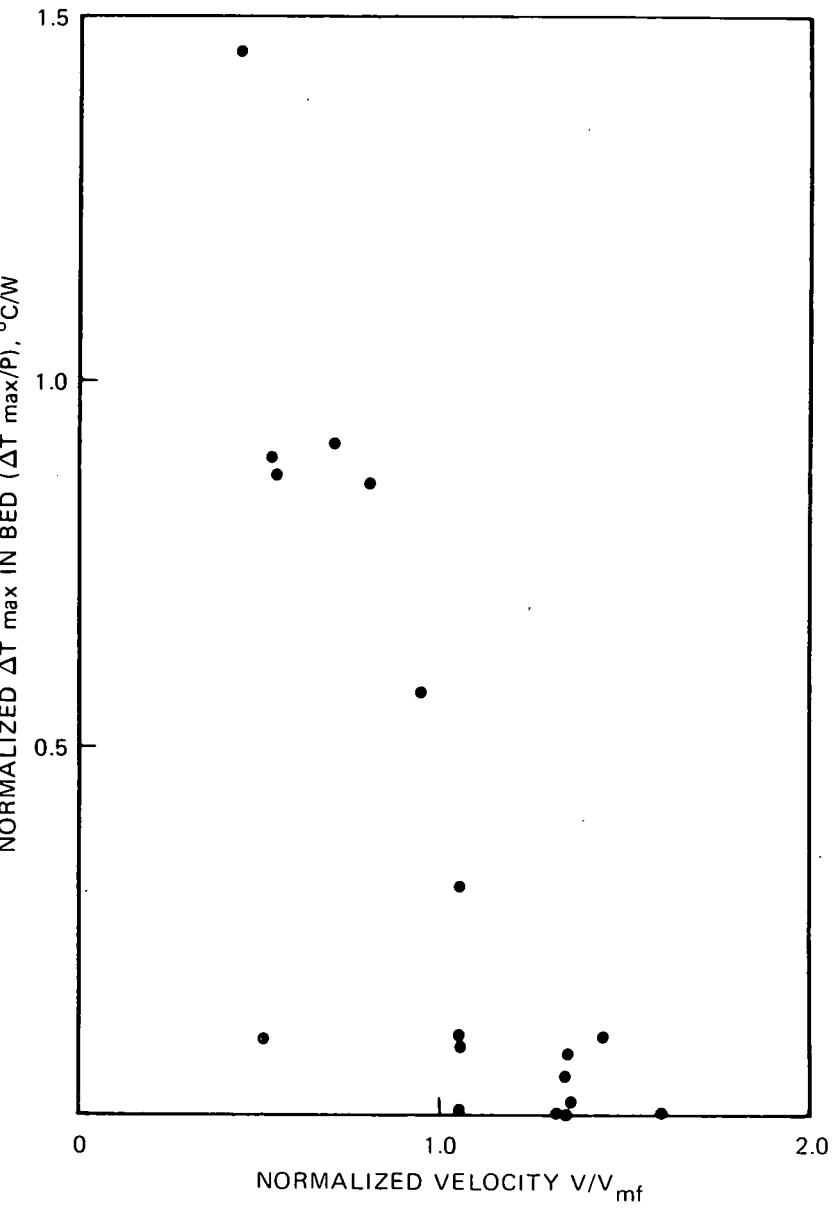


Figure 4.10
MAXIMUM TEMPERATURE DIFFERENCE IN BED
NORMALIZED TO INPUT POWER vs FLOW VELOCITY
NORMALIZED TO MINIMUM FLUIDIZATION VELOCITY

Numerous tests were conducted to measure the bed temperature under various conditions. As would be expected, the temperatures at different points within the bed are substantially equal when the bed is fluidized, and much different when the bed is packed as shown in Figure 4.10.

4.3 CONCLUSIONS

The analytical model suggests the following: the critical silane concentration increases with decreasing particle temperature. Therefore, the bed should be operated at a low temperature ($\sim 950^{\circ}\text{K}$) if the product morphology is acceptable. Around this temperature, the power input and the reactor size are both reasonable. In the temperature range of interest, these conclusions can be made whether heating is to the gas or directly to the bed particles.

Experimental work shows that the measured minimum fluidization velocities agree quite well with the predicted values. We were able to match the electrical power input to the bed with the measured power output (thermal). The temperature measurements throughout the bed showed that the bed temperature variation is negligible when the bed is fluidized as predicted and that the temperature difference was quite substantial when the bed was packed.

4.4 PROJECTED QUARTERLY ACTIVITIES

4.4.1 EXPERIMENTAL INVESTIGATION

All experimental work will be completed in April and the results will be documented.

4.4.2 ANALYTICAL WORK

Based on the analytical model and the experimental findings, various attractive fluid-bed pyrolysis schemes will be studied. A functional process design of the base case and the economic analysis will be completed.